Doctoral Dissertation

Dynamical neural activities in hippocampus and auditory cortex during the learning process of an associative memory task

Shogo Takamiya

Graduate School of Brain Science, Doshisha University

Abstract

Associative learning is the process by which stimuli and behavior become associated with being experienced and reinforced. For successful associative learning, neural circuits integrate stimulus information with responses. Hippocampus is thought to be the area that integrates stimuli with behavior. During behavioral acquisition, the hippocampus rapidly encodes information via changes in synaptic strength. Then the information is repeatedly replayed during slow-wave sleep and transferred to the neocortex for consolidation. Thus, associative memory becomes independent of hippocampal function when consolidated and stored in neocortical neuronal circuits. However, it is unclear how the activities of hippocampal and neocortical neurons dynamically change during the learning process, in which associative memory is gradually formed. To investigate this issue, we developed an associative memory task using auditory stimuli for rats. In this task, rats were required to associate tone frequencies (high and low) with a choice of ports (right or left) to obtain a reward. The activity of hippocampal CA1 and primary auditory cortex (A1) neurons in the rats during the learning process of the task was recorded. Many hippocampal CA1 neurons increased their firing rates when the rats received a reward after choosing either the left or right port. We referred to these cells as “reward-direction cells.” Furthermore, the proportion of reward-direction cells increased in the middle-stage of learning but

decreased after the completion of learning. In contrast, many A1 neurons increased their firing rates when the rats were presented with a high or low tone (frequency-selective cells). Furthermore, reward-direction cells were also observed in A1. The proportion of frequency-selective and reward-direction cells increased with task acquisition and reached the maximum level in the last stage of learning. The results of hippocampal CA1 neurons suggest that the activity of reward-direction cells might serve as a "positive feedback" signal that facilitates the formation of associations between tone pitches and port choice. The results of A1 neurons suggest that they have a task- and learning-dependent selectivity toward sensory input and reward when auditory tones and behavioral responses are gradually associated during task training. This selective activity of A1 neurons may facilitate the formation of associations, leading to the consolidation of associative memory. Collectively, our results indicate that the hippocampus and auditory cortex interact with each other, and the interaction between them plays an important role in memory formation and leads to consolidation.

Acknowledgment

I would like to express my deepest gratitude to my supervisor, Dr. Yoshio Sakurai, for his continuous guidance, scientific advice, and encouragement during the last five years. I also thank Dr. Junya Hirokawa, Dr. Hiroyuki Manabe, and the past and present lab members for their encouragement and insightful comments on this research. I want to give special thanks to members of my thesis committee, Dr. Susumu Takahashi, Dr. Jun Motoyama, and Dr. Yoshito Masamizu, for their time and efforts in my examination. I am also grateful to the Japan Society for the Promotion of Science (JSPS) and Doshisha University for their financial support. Finally, I wish to extend my sincere gratitude to my family for their understanding, support, and encouragement. I would not have been able to complete this study without their dedication.

Table of contents

Chapter 1. Introduction 11

1.1 Associative learning 11

1.2 Neural activity in the hippocampus during associative learning 16

1.3 Neural activity in the auditory cortex during associative learning 18

1.4 Anatomical connectivity between the hippocampus and auditory cortex. 19

1.5 Aim of this study 21

Chapter 2. Materials and Methods 22

2.1 Subjects 22

2.2 Apparatus 22

2.3 Behavioral task 24

2.4 Surgery 27

2.5 Recording 27

2.6 Histology 29

2.7 Spike sorting 29

2.8 Cell classification 31

2.9 Data analysis 31

2.9.1 Spike train analysis 31

2.9.2 ROC analysis 32

2.9.3 Detecting task-related neurons in hippocampal CA1 33

2.9.4 Detecting task-related neurons in A1 34

2.9.5 Quantifying the degree of selectivity 36

2.10 Statistical analysis 36

Chapter 3 Results 38

3.1 Hippocampal CA1 neurons show task-related and learning-dependent activity 38

3.1.1 Learning of the associative memory task and cell classification of hippocampal CA1 neurons 38

3.1.2 Choice-direction selective activity of CA1 pyramidal neurons 44

3.1.3 Reward-direction selective activity of CA1 pyramidal neurons 46

3.2 Auditory cortex neurons show task-related and learning-dependent activity 49

3.2.1 Learning of the associative memory task and recording of neural activity from A1 . 49

3.2.2 Frequency-selective activity of A1 neurons 55

3.2.3 Frequency-selective activity engagement in the task 57

3.2.4 Choice-direction selective activity of A1 neurons 59

3.2.5 Reward-direction selective activity of A1 neurons 61

Chapter 4 Discussion 65

4.1 Hippocampal CA1 neurons represent positive feedback during learning process 65

4.2 Auditory cortex neurons show learning-dependent selectivity toward not only sound input but also rewards 69

4.3 Interaction between hippocampus and auditory cortex during learning process 74

4.4 Study limitation and future plan 77

4.5 Outlook 78

References 79

List of Figures and tables

Figures

Figure 1. Schematic drawing of classical and operant conditioning.

Figure 2. Schematic drawing illustrating components of associative learning.

Figure 3. Schematic diagram of anatomical connectivity between the hippocampus and auditory cortex.

Figure 4. Pictures of an operant chamber.

Figure 5. Associative memory task.

Figure 6. Schematic drawing of the recording procedure.

Figure 7. Examples of sorted neurons from a tetrode on successive recording sessions.

Figure 8. Behavioral performance and recording of neural activity in the hippocampal CA1.

Figure 9. Cell classifications.

Figure 10. Proportion and selectivity of choice-direction cells in hippocampal CA1 during learning.

Figure 11. Proportion and selectivity of reward-direction cells in hippocampal CA1 during learning.

Figure 12. Task performance and recording of neural activity in the A1.

Figure 13. Proportion and selectivity of frequency-selective cells in the A1 during

learning.

Figure 14. Comparison of the neural activity between the task and passive tone condition.

Figure 15. Proportion and selectivity of choice-direction cells in the A1 during learning.

Figure 16. Proportion of reward-direction selective cells in the A1 during learning.

Figure 17. Summary of the results in this study.

Tables

Table 1. Task performance (percent correct) of each rat while recording the hippocampal neural activity during each session.

Table 2. Number of sessions required for each rat for recording of hippocampus to acquire the task.

Table 3. Number of pyramidal neurons (all neurons) in the hippocampal CA1 recorded in each rat during each session.

Table 4. Numbers of task-related cells and conjunctive cells in hippocampal CA1 in each learning stage.

Table 5. Task performance (percent correct) of each rat for recording of A1 in each session.

Table 6. Number of sessions required for each rat for recording of A1 to acquire the task.

Table 7. Number of neurons in the A1 recorded in each rat during each session.

Table 8. Numbers of task-related cells and conjunctive cells in the A1 in each learning stage.

Chapter 1. Introduction

1.1 Associative learning

Associative learning is the process in which stimuli and behavior become associated with being experienced and reinforced. This learning can be classified into two types of conditioning, i.e., classical conditioning and operant conditioning. Classical conditioning is referred to as automatic or passive learning. In this type of conditioning, an initially neutral stimulus (conditioned stimulus, CS) that precedes a stimulus (unconditioned stimulus, US) eliciting a response (unconditioned response, UR) becomes to function as a predictor of the US. Following the association between CS and US, the animal produces an anticipatory response (conditioned response, CR) that resembles UR when presented with the CS (Baxter DA & Byrne JH, 2006). This association between CS and CR occurs involuntarily and unconsciously (Figure 1A). Operant conditioning, on the other hand, is referred to as voluntary and conscious learning. In this conditioning, an animal learns to anticipate positive (reward) or negative (punishment) consequence that consistently occurs as a result of the animal's own behavior (Skinner, 1937). Rewards play a role as "reinforcement," which strengthens or increases the behavior it follows, but punishment causes a decrease in the behavior it follows (Figure 1B). The brain mechanisms of classical and operant conditioning are supposed to be different because their learning processes are different. Memories of classical conditioning might be

localized in one brain region; on the other hand, those of operant conditioning might be represented by networks of several brain regions (Squire, 1987).

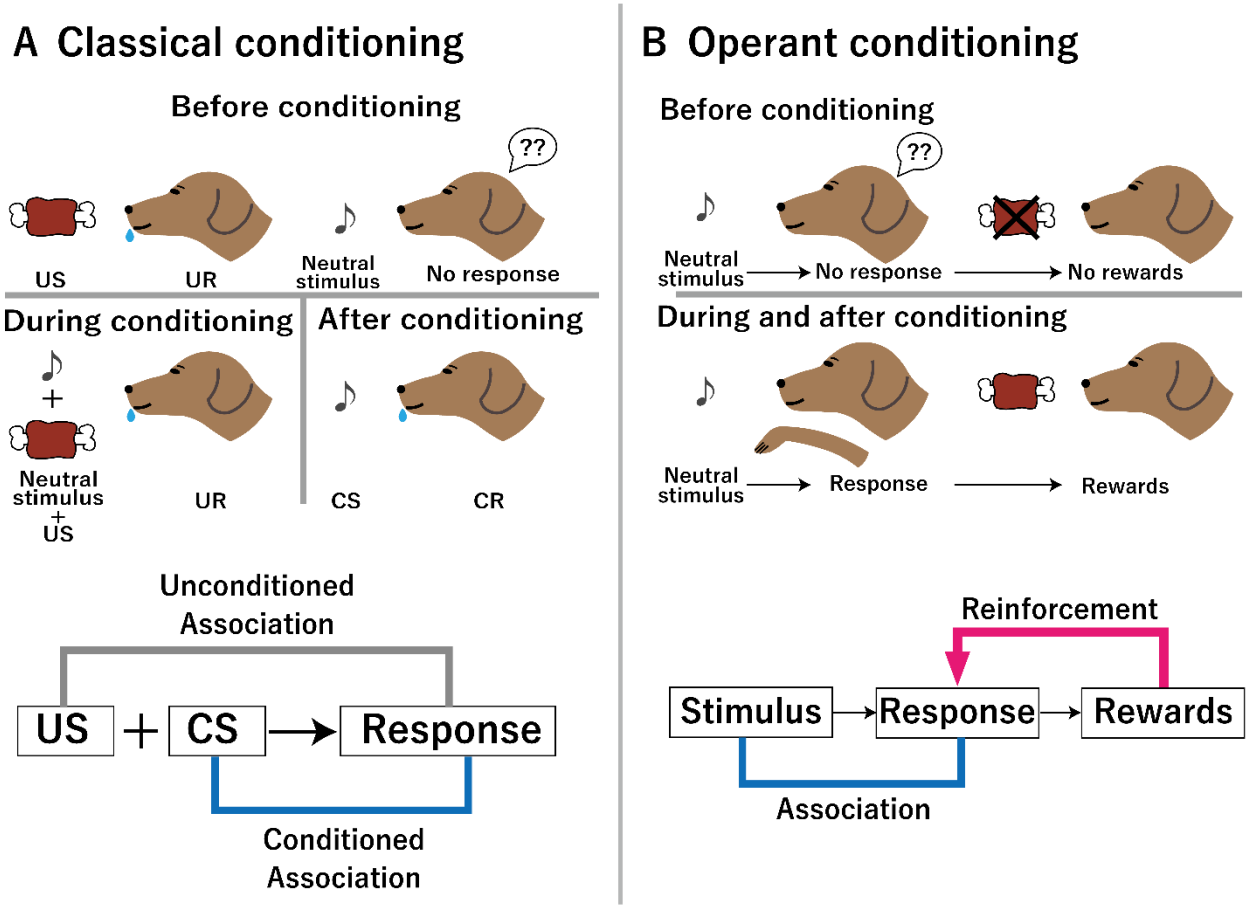

Figure 1. Schematic drawing of classical and operant conditioning.

(A) Schematic example of classical conditioning. US, unconditioned stimulus; UR, unconditioned response; CS, conditioned stimulus; CR, conditioned response. An animal shows no response to a neutral stimulus (CS) before conditioning. During conditioning, CS and US are presented simultaneously, and the animal shows a specific response (UR) to US. It causes an association between CS and UR, and presenting only CS but not US induces an anticipatory response (CR) after conditioning. (B) Schematic example of operant conditioning. This example shows positive reinforcement conditioning. An animal can get rewards when it shows a specific response to a neutral stimulus. Before conditioning, the animal shows no response to the stimulus. During conditioning, the animal shows different kinds of responses to the stimulus to get rewards. The animal increases those responses that yield rewards. The association between the stimulus and the response is formed by rewards which play a role as a reinforcer.

Previous studies have used different types of conditioning to reveal the neural activity in the various brain regions in associative learning. For successful associative learning, neural circuits integrate stimulus information with responses (Figure 2). The hippocampus is thought to be the area that integrates stimuli with behavior (Eichenbaum et al., 1987; Sakurai, 1996; Sakurai, 1990, 1996). In addition, it is also important that sensory regions corresponding to the various stimulus types modulate their neural activity during learning processes (Weinberger, 2004).

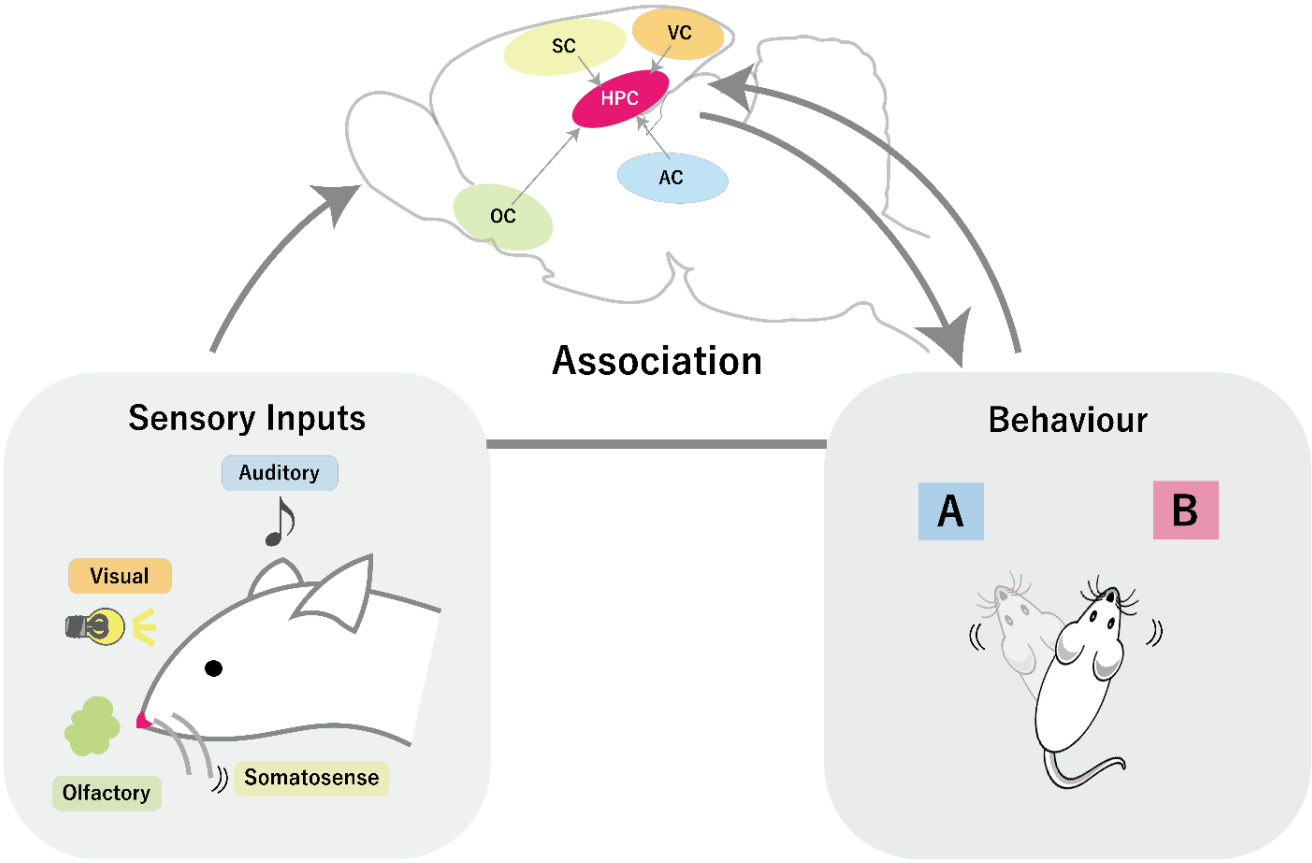

Figure 2 Schematic drawing illustrating components of associative learning.

The hippocampus is thought to be the area that integrates stimulus with behavior. This region receives inputs from the different parts of the sensory cortex. The interaction between the sensory cortex and the hippocampus creates an association between stimulus and behavior. SC: somatosensory cortex, VC: visual cortex, AC: auditory cortex, OC: olfactory cortex.

1.2 Neural activity in the hippocampus during associative learning

Associative learning forms and consolidates associative memory. The hippocampus plays a critical role in encoding spatial memory (O'keefe and Nadel, 1978; McNaughton et al., 2006) and associative memory that associates olfactory (Eichenbaum et al., 1987), visual (Sakurai, 1996), and/or auditory (Sakurai, 1990, 1996) information in addition to spatial information. Associative memory becomes independent of hippocampal function when consolidated (Eichenbaum, 2000; Frankland et al., 2005). According to the two-stage model (Buzsaki, 1996, 2015), the hippocampus rapidly encodes information via changes in synaptic strength during behavioral acquisition, and then the information is repeatedly replayed during slow-wave sleep and transferred to the neocortex for consolidation. Certainly, hippocampal lesions cause impairment in associative memory, but they do not affect the memory already formed by sufficient training (Tse et al., 2007). Recent studies utilizing optogenetics have revealed that the reactivation of neurons in the hippocampus is necessary for the retrieval of "recent" memory, while the reactivation of neurons in the neocortex is necessary for the retrieval of "remote" memory (Kitamura et al., 2017). However, optogenetic experiments used classical conditioning, i.e., simple behavioral tasks using reflex responses that can be learned in a single experience (trial), such as contextual fear conditioning. Therefore, it is unclear how the neural activities of hippocampal neurons dynamically change during the learning process using operant conditioning, in which associative memory is gradually

modified from recent and unstable memory to a stable one over a longer period.

Hattori et al. (2015) addressed this exact question using chronic electrophysiology and trace conditioning of the eyeblink reflex in rabbits. They revealed the learning-specific activity of hippocampal neurons in both the acquisition and retrieval of associative memories. The present study aimed to address the same question as Hattori et al. (2015) did. However, this study used operant conditioning with rewards in an associative memory task that was gradually learned over several days. Moreover, this study investigated changes in the activities of hippocampal CA1 and sensory cortical neurons during the learning process of the associative memory task and discussed the different roles of the hippocampus and the sensory cortex for the formation of associative memory.

1.3 Neural activity in the auditory cortex during associative learning

Associative learning between stimuli and behavioral responses induces modulation of neural activity in several brain regions. For successful associative learning, neural circuits integrate stimulus information with the correct choices and rewards. This means that sensory regions, besides the hippocampal and motor regions, modulate their neural activity during learning processes (Weinberger, 2004). During learning with auditory stimuli, A1 neurons, each of which intrinsically responds to a specific tone frequency (tonotopic representation), become tuned to the frequency of the conditioned tone, and the proportion of these neurons increases with training (Bakin and Weinberger, 1990; Weinberger, 2004). Thus, A1 neurons have high plasticity, and their firing preference is modulated by auditory associative learning (Irvine, 2017).

The activity of A1 neurons is modulated not only by inputs but also by other task-related variables (Lin et al., 2019; Caras and Sanes, 2017). Guo et al. (2019) reported that A1 neurons show choice-direction selectivity, whereas Bigelow et al. (2019) reported that motor movements modulate A1 neuronal activity. Furthermore, reward-related activity has been detected in A1 neurons (Brosch et al., 2011). Therefore, it is likely that A1 neurons represent important variables related to associative memories that form relations between auditory stimuli, behavioral choices, and rewards. However, neural recordings for A1 could not uncover their modulation during the learning process of an

associative memory task, and it is unclear how A1 neural activity changes dynamically in response to these variables during the learning processes related to associative memory tasks.

1.4 Anatomical connectivity between the hippocampus and auditory cortex.

The connectivity between the hippocampus and auditory cortex is very complicated and has several pathways (Figure 3). For instance, the hippocampus receives auditory input from the entorhinal and perirhinal cortex (Mohedano-Moriano et al., 2007; Munoz-Lopez et al., 2010). In turn, the auditory cortex receives inputs from the hippocampus via the entorhinal or perirhinal cortex (O'Mara, 2005). Moreover, there is a direct pathway from the hippocampus to the auditory cortex in rodents (Cenquizca and Swanson, 2007). However, few studies have investigated modulations and interactions of neural activities between the hippocampus and auditory cortex during associative learning.

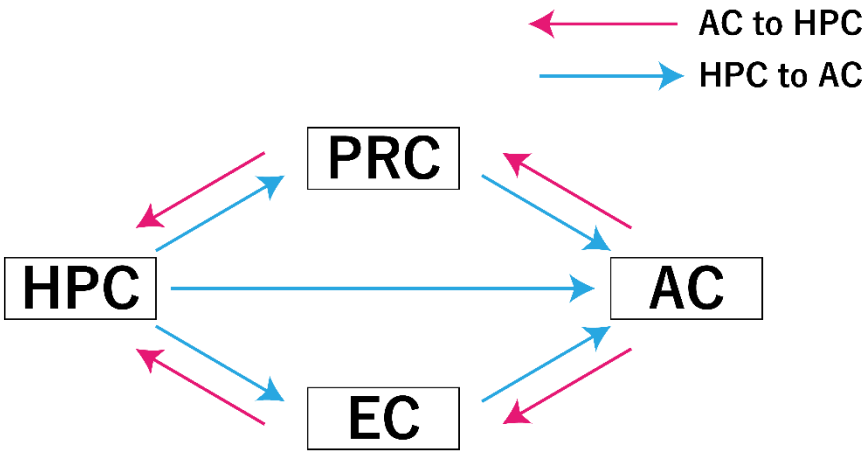

Figure 3. Schematic diagram of anatomical connectivity between the hippocampus and auditory cortex.

Pink arrows indicate the pathway from the auditory cortex to the hippocampus. Blue arrows indicate the pathway from the hippocampus to the auditory cortex. HPC, hippocampus; EC, entorhinal cortex; PRC, perirhinal cortex; AC, auditory cortex.

1.5 Aim of this study

Associative learning may induce modulations of neural activities in the hippocampus and sensory cortex. However, it is unclear how the activities of hippocampal and sensory cortical neurons dynamically change during the process of learning an associative memory task. The aim of this study is to elucidate the modulation of neural activities in hippocampal CA1 and A1 throughout the learning process that occurs during an associative memory task. Therefore, we developed an auditory associative memory task for rats, in which associative memory is gradually acquired over several days. In this task, the rats were required to associate tone pitches (high and low) and ports (right and left) to obtain rewards. We recorded the firing activity of neurons in rat hippocampal CA1 and A1 during some days of the learning process of the task. We hypothesized that the number of task-related neurons in the hippocampal CA1 might increase when the rats were beginning to learn the task and decrease when they had learned it, and, on the other hand, the number of task-related cells in the A1 gradually increased, that is, their firing was gradually modulated during the completion of the task.

Chapter 2. Materials and Methods

2.1 Subjects

A total of thirteen male Wistar albino rats (twelve to fifteen weeks old: Shimizu Laboratory Supplies, Kyoto, Japan) were used in this study: seven for electrophysiological recordings from the hippocampal CA1 area and six for auditory cortex recordings. All rats were individually housed and maintained on a laboratory light/dark cycle (lights on at 8:00 and off at 21:00). The rats were placed on food restriction with ad libitum access to water and maintained at approximately 80% of their baseline weight throughout the experiments. All experiments were conducted following the guidelines for the care and use of laboratory animals provided by the Animal Research Committee of Doshisha University.

2.2 Apparatus

Behavioral training was performed in an operant chamber (23 × 11 × 35 cm; Ohara-Ika, Tokyo, Japan) with two ports in the front wall and a port in the back wall for a nose-poke response (Figure 4). The distance between the right and left ports was 70 mm. Each port was equipped with an LED light and an infrared sensor, which detected the nose-poke responses in the animal. A loudspeaker (15 cm in diameter) was placed 15 cm above the top of the chamber for the sound stimuli. A food dispenser delivered a 45 mg

food pellet to a magazine located 1.5 cm above the floor and in the middle of the front wall. The chamber was enclosed in a soundproof box (Brain Science Idea; Osaka, Japan). All the events were controlled using a personal computer (NEC, Tokyo, Japan).

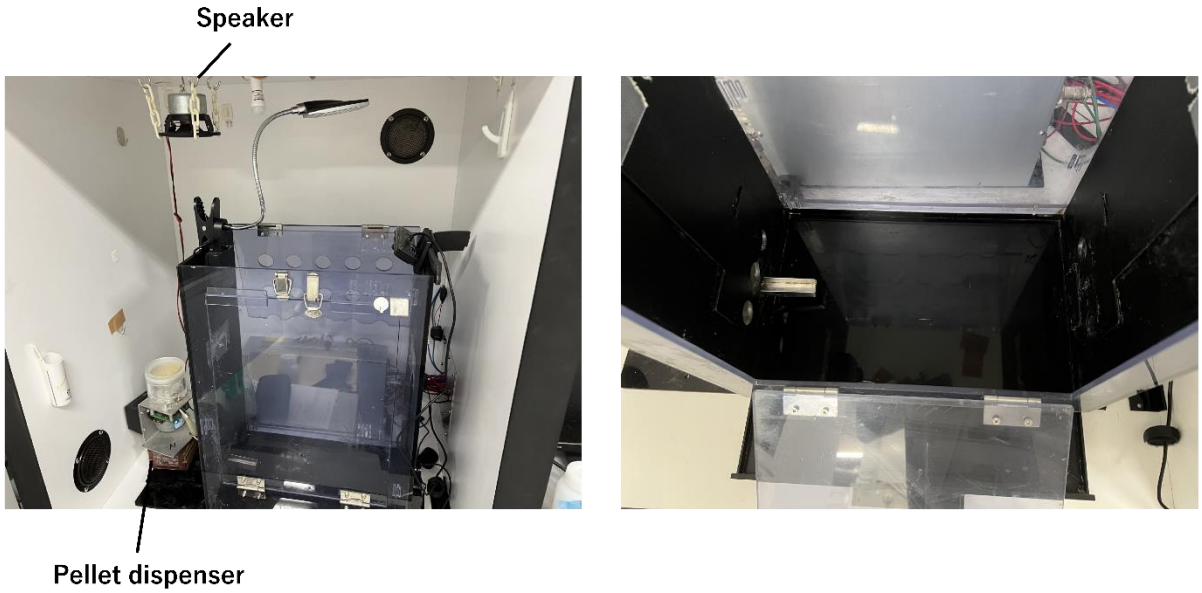

Figure 4. Pictures of an operant chamber.

Behavioral training was performed in an operant chamber enclosed in a soundproof box (left). It has two ports and a reward magazine on the front wall and a port on the back wall for a nose-poke response (right). Each port was equipped with an LED light and an infrared sensor, which detected the nose-poke responses in the animal. A loudspeaker was placed above the top of the chamber for the sound stimuli. A food dispenser delivered a 45 mg food pellet to a magazine located above the floor and on the middle of the front wall.

2.3 Behavioral task

The rats were trained in an associative memory task with tones, in which they were required to associate tone frequencies (high and low) and port locations (right and left) (Figure 5). All animals learned the task with the same rule; that is, they learned a high tone-right reward association and a low tone-left reward association. At the start of each trial, the port in the back wall was lit, and a high or low tone was randomly presented when the rat poked its nose into the port. Subsequently, the light in the port on the back wall was turned off, and the lights in the right and left ports on the front wall were turned on. When the tone was high, it was correct for the rat to poke its nose into the right port. When the tone was low, the correct response was to choose the port on the left. Immediately after the choice response, the light from the ports in the front wall turned off. A food pellet was delivered into the pellet magazine along with a buzzer noise when the rat made the correct choice, and the port in the back wall was lit again to start the next trial. When the rat chose incorrect ports, a timeout was imposed, and the lighting on the back wall port to start the next trial was delayed for 5 s. When the rat did not choose either the right or left port for 10 s, the trial was canceled. The selection of high or low tones was pseudo-random, long runs of more than four successions of one type of tone were not permitted, and there was an equivalent number of high-and low-tone trials in each session.

The rats were trained with 3 kHz and 1 kHz tone stimuli until their accuracy reached

over 80%. After completion of the training, the rats underwent surgery for electrode implantation. A week after surgery, the rats were trained in the same task, but the tone stimuli were 10 kHz and 6 kHz. They were trained until the choice accuracy was over 80 %, and we recorded all neural activity during the training process. Each training session consisted of 150–250 trials per day.

Three of the six rats used for auditory cortex recordings performed a passive tone conditioning task after completing the training in the associative memory task. The rats were randomly exposed to 3 s of 10 kHz and 6 kHz tones presented 50 times each at 20 s intervals in the operant chamber.

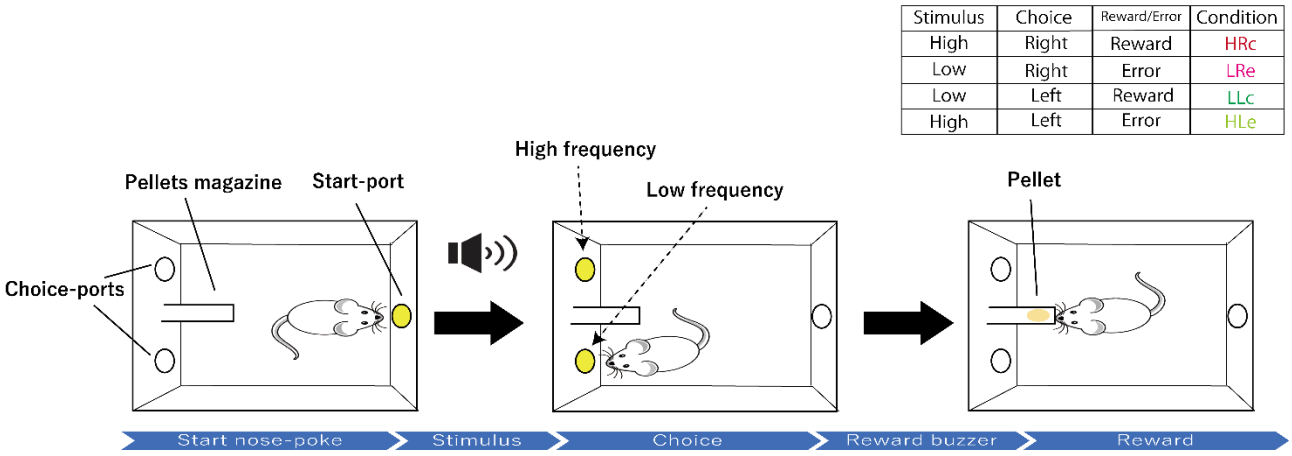

Figure 5. Associative memory task.

Schematic representation of an associative memory task. In this task, the rats were required to associate tone frequencies (high and low) and port locations (right and left). At the start of each trial, a high or low tone was randomly presented when the rat poked its nose into the start port. When the tone was high, it was correct for the rat to poke its nose into the right port. When the tone was low, the correct response was to choose the port on the left (top panel). A food pellet was delivered into the pellet magazine along with a buzzer noise when the rat made the correct choice. When the rat chose incorrect ports, a timeout was imposed, and the lighting on the back wall port to start the next trial was delayed for 5 s.

2.4 Surgery

The rats were anesthetized with 2.5% isoflurane before surgery, which was maintained throughout the surgical procedure. We monitored the rats' body temperature and depth of anesthesia as needed. An eye ointment was used to keep the animals' eyes moistened throughout the surgery. A craniotomy was performed over the right hippocampus (AP, -3.2 to -3.0 mm, ML, 2.2 to 2.5 mm relative to the bregma, 1.5 mm below the brain surface) in seven rats and the right auditory cortex (AP, -5.5 to -5.4 mm, ML, 6.7 to 7.2 mm relative to the bregma, 1.0 mm below the brain surface) in six rats, and custom-designed tetrodes attached to a microdrive were vertically implanted using a stereotactic manipulator. A stainless-steel screw was placed over the cerebellum and served as the ground during the recording.

2.5 Recording

For each rat, eight tetrodes composed of four tungsten wires (12.5 μm, California Fine Wire, Grover Beach, CA) were used for extracellular recordings (Figure 6). Each tetrode was covered by a polyimide tube (A-M Systems, Sequim, WA, USA) and placed 100 μm apart. The tip impedance was 200–1000 kΩ at a frequency of 1 kHz. The signals were recorded using a head stage (Intan Technologies, USA) and a multichannel electrophysiology acquisition board (Open Ephys, Cambridge, MA) at a sampling rate

of 30 kHz and bandpass filtered between 0.3 kHz and 6 kHz. The mean activity of all the tetrodes was used as a reference. During a week of postsurgical recovery, the tetrodes were advanced by 20 μm per day until the firing of some cells was observed. We did not move the tetrodes during the training of the rats to record the same cell population throughout the training process.

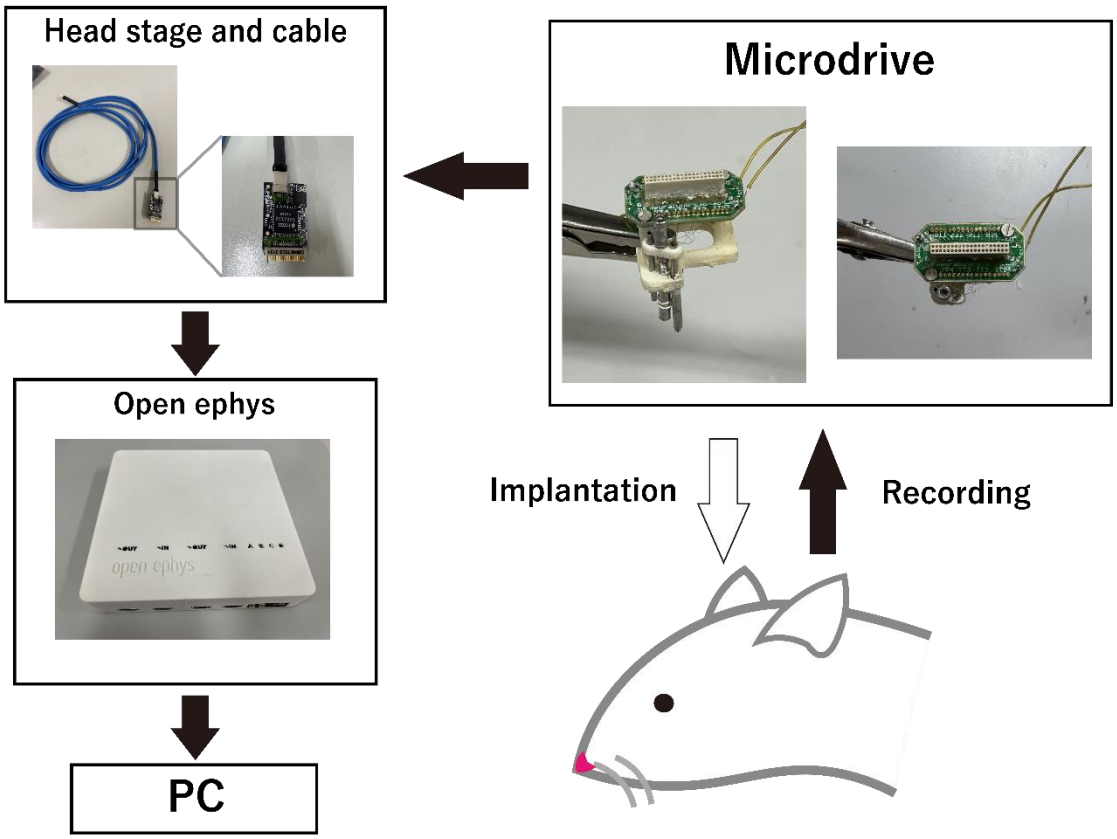

Figure 6. Schematic drawing of the recording procedure.

A microdrive attaching eight tetrodes was implanted into rats' brains (top and bottom, right). The signals from rats' brains were recorded using a head stage (left top) and a multichannel electrophysiology acquisition board (left middle).

2.6 Histology

After the experiment, each rat was anesthetized with sodium pentobarbital and perfused with phosphate-buffered saline and 4 % paraformaldehyde. The brains were removed and post-fixed in 4 % paraformaldehyde, and 50 μm coronal sections of the brains were prepared to confirm the recording sites.

2.7 Spike sorting

Spike sorting analysis was performed using MATLAB software (MathWorks, Natick, MA, USA). To detect single neuron activity, spikes were manually clustered based on their waveform energy, peak amplitude, and first principal components from four channels with MClust (A.D. Redish; https://redishlab.umn.edu/mclust) in MATLAB. Only those neurons that met the following criteria were included for further analyses: (1) the isolation distance, which was estimated as the distance from the center of the identified cluster to the nearest cluster on the basis of the Mahalanobis distance, was greater than 15 (Schmitzer-Torbert et al., 2005; Jackson et al., 2006) and (2) spikes with reliable refractory periods of 2 ms (violations were < 1 % for all spikes).

The constant-spike waveforms of the individual neurons were confirmed within a single session. The spike waveforms were also stable in repeated recordings on successive days (Figure 7).

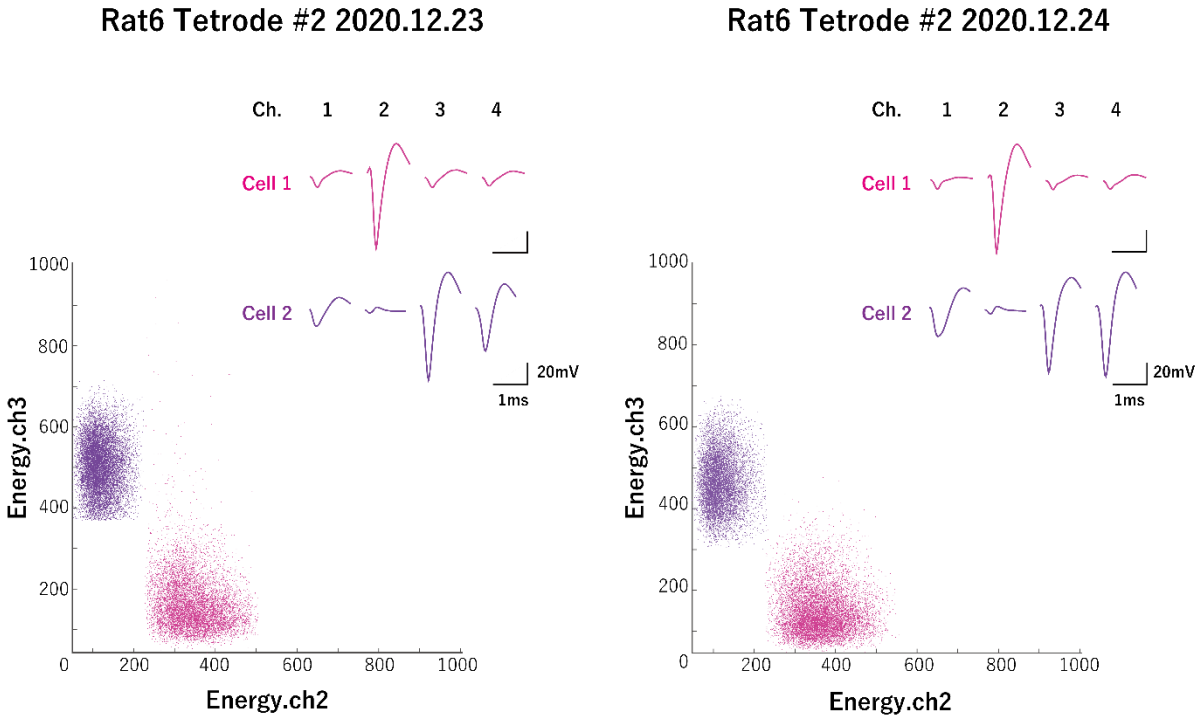

Figure 7. Examples of sorted neurons from a tetrode on successive recording sessions.

Top panels show the averaged spike waveforms of cell 1 and 2 in the hippocampal CA1 on each channel of tetrode # 2. Bottom scatter plots show the spike clusters during the first and second sessions. Each dot represents a spike. The horizontal and vertical axes represent the energy of the spikes as detected by channels 2 and 3 of tetrode # 2, respectively. Clusters and waveforms, represented by different colors, indicate different single-neuron.

2.8 Cell classification

We classified hippocampal CA1 neurons based on their trough-to-peak width. Cells with trough-to-peak width equal to or greater than 0.4 ms and less than 0.4 ms were defined as putative pyramidal neurons and interneurons, respectively.

2.9 Data analysis

2.9.1 Spike train analysis

We computed peri-stimulus time histograms using a 20 ms bin width and smoothed them by convolving spike trains with a 40 ms wide Gaussian filter in the following four trial outcome conditions: high-right-correct (HRc), low-right-erroneous (LRe), low-left-correct (LLc), and high-left-erroneous (HLe). To examine the relationship between firing rate modulation and the development of behavioral epochs in the behavioral task, we used event-aligned spike histograms (EASHs). As the choice epoch durations varied for each trial, the median duration from the time when the stimulus was presented to when the rats chose either port was calculated. The median time from rats for hippocampal CA1 area recordings was 2.17 s, and the time from rats for A1 area recordings was 2.38 s. The spike timing during the choice epoch of each trial was linearly transformed into the median duration.

2.9.2 ROC analysis

To quantify firing rate changes, we used an algorithm based on an area under the receiver operating characteristic curve analysis (auROC) that calculates the ability of an ideal observer to classify whether a given spike rate was recorded in one of two conditions (Green and Swets, 1996; Felsen and Mainen, 2008). For each neuron, we performed auROC analysis. Starting from the baseline period of each condition (1 s of fixation before the start of the trial), the ROC value was calculated for each 100 ms bin. This bin was then advanced in 20 ms increments until 5 s after the trial began. We also performed auROC analysis to evaluate the selectivity of each neuron by comparing the firing rate of each trial condition (HRc vs. LRe, HRc vs. HLe, HRc vs. LLc, LLc vs. HLe, LLc vs. LRe, and HLe vs. LRe) in the same manner as described previously. We used permutation tests (1,000 iterations) to determine the statistical significance ($p < 0.05$ for recording data from the hippocampal CA1; $p < 0.01$ for recording data from A1). auROC values were defined as $2 \times (\text{auROC curve} - 0.5)$, ranging from -1 to 1. The sample size for the test was no fewer than eight trials. This is sufficient because the minimal sample size used in a previous study was four trials (Felsen et al., 2008).

2.9.3 Detecting task-related neurons in the hippocampal CA1

We defined two types of task-related neurons in the hippocampal CA1 under the following conditions:

Choice-direction cells were defined to have the following characteristics :(1) auROC values of the HRc or LLc that were calculated by comparing the firing rates of each period to the baseline of each condition were significant for five bins in a row in the period from the trial started to the points of choice response; (2) auROC values of HRc *vs.* LLc that were calculated by comparing the firing rates of the HRc trials to those of the LLc trials were significant for the same periods as (1).

Reward-direction cells were definedto have the following characteristics: (1) either the auROC values of the HRc trials or that of the LLc trials that were calculated by comparing the firing rates of each period to the baseline of each condition were significant for five bins in a row in the period from choice response to the time after 3 s from choice response; (2) auROC values of the HRc (LLc) trials that were calculated by comparing the firing rates of the HRc (LLc) trials to that of the other trials were significant for the same periods as (1).

We detected neurons that responded to two events (choice direction and reward direction), and each conjunctive cell was counted twice for each response type (Table 4).

2.9.4 Detecting task-related neurons in the A1

We defined several task-related neurons under the following conditions:

Frequency-selective cells modulated their firing rates in response to tonal differences (high or low). These cells consist of high- and low-frequency selective cells. High-frequency selective cells were characterized by : (1) auROC values of HRc vs. LLc that were significant for five bins in a row from the start of the trial to the points of choice. (2) The auROC values of HRc vs. LRe that were significant for the same period as in (1) (3) The auROC values of HRc vs. HLe that were not significant for the same period as in (1)

We defined low-frequency selective cells as having the following features: (1) auROC values of LLc vs. HRc that were significant for five bins in a row from the start of the trial to the points of choice. (2) The auROC values of LLc vs. HLe that were significant for the same period as in (1) (3) The auROC values of LLc vs. LRe that were not significant for the same period as in (1)

Sound-evoked cells: The auROC values of all conditions were calculated by comparing the firing rates of each period to the baseline of each condition that was significant for five bins in a row from the start of the trial up to 1 s after the response.

Choice-direction cells modulated their firing rates in response to the choice of direction (right or left). These cells consisted of right- and left-choice selective cells. We defined

right-choice selective cells as being characterized by: (1) the auROC values of HRc vs. LLc that were significant for five bins in a row from the start of the trial to the points of choice. (2) The auROC values of HRc vs. HLe that were significant for the same period as in (1)　(3) The auROC values of HRc vs. LRe that were not significant for the same periods as in (1)

We defined left-choice selective cells as having : (1) the auROC values of LLc vs. HRc that were significant for five bins in a row from the start of the trial to the points of choice. (2) The auROC values of LLc vs. LRe that were significant for the same period as in (1)　(3) The auROC values of LLc vs. HLe that were not significant for the same period as in (1)

Reward-direction selective cells modulated their firing rates after the rats chose either of the correct ports (left or right). These cells consist of right-choice reward selective cells and left-choice reward selective cells. We defined right-choice reward selective cells as having the following features: (1) auROC values of HRc vs. LLc that were aligned by choice response time and were significant for five bins in a row from the time of choice to 3 s after the response. (2) The auROC values of HRc vs. LRe that were aligned by choice response time and were significant for the same periods as in (1)　(3) The auROC values of HRc vs. HLe that were aligned by choice response time and were significant for the same periods as in (1).

We defined left-choice reward selective cells as having the following attributes: (1) The auROC values of LLc vs. HRc that were aligned by choice response time and were significant for five bins in a row from the time of choice to 3 s after the response. (2) The auROC values of LLc vs. LRe that were aligned by the choice response time and were significant for the same periods as in (1). (3) The auROC values of LLc vs. HLe that were aligned by choice response time and were significant for the same periods, as in (1).

We detected a few neurons that responded to two or three events (frequency, choice-direction, and reward-direction), and each conjunctive cell was counted twice or thrice for each of the three response types (Table 8).

2.9.5 Quantifying the degree of selectivity

We computed a selectivity index to evaluate the degree of selectivity, which was calculated as "(H – L)/(H + L)." H and L are the average firing rates of the HRc and LLc trials in 100 ms around the selectivity peak, respectively.

2.10 Statistical analysis

Behavioral performance: One-way ANOVA and multiple comparison tests were used to compare differences in task performance.

Detecting task-related cells: We used auROC analysis and permutation tests because it is usually difficult to predict the type (normal or non-normal) of the distribution of neuronal firing rates and populations of task-related neurons (Sakurai, 1994; 1996). Therefore, our past and recent studies (Sakurai, 1994,1996; Shiotani et al., 2020; Tanisumi et al., 2021; Ohnuki et al., 2020; Osako et al., 2021) used distribution-free nonparametric statistics (Siegel, 1956) or ROC analyses (Green and Swets, 1996) rather than parametric analyses (e.g., ANOVA) to analyze neuronal firing rates statistically and to define task-related activity. auROC analysis has an advantage in that we can compare differences between conditions quantitatively using auROC values, whereas we cannot compare them quantitatively with *p*-values in an ANOVA.

Proportions of task-related cells: The chi-squared test was used for group effects, and Fisher's exact test was used to detect a significant difference between the two conditions. The tally from Fisher's exact test was corrected using Holm correction. Strength of selectivity: Selectivity index comparisons between two conditions and among three conditions were analyzed using the Wilcoxon rank-sum and Kruskal–Wallis tests, respectively.

Chapter 3 Results

3.1 Hippocampal CA1 neurons show task-related and learning-dependent activity

3.1.1 Learning of the associative memory task and cell classification of hippocampal CA1 neurons

Seven rats were trained in the associative memory task with frequencies of 3 kHz and 1 kHz as pre-training. The rats performed the task in two to seven sessions (days). The electrodes were implanted when the rats completed the pre-training. A week after the surgery for electrode implantation, the rats began to learn the task at frequencies of 10 kHz and 6 kHz (learning sessions). The rats completed the task in three to five sessions (days) (Tables 1 and 2). We divided the learning sessions into three stages (Figure 8A). We defined the first session as the "early-stage" (mean behavioral accuracy=57.7%, n=7) and the last session as the "late-stage" (mean behavioral accuracy=84.29%, n=7). We also defined the sessions before the last session as the "middle-stage" (mean behavioral accuracy=73.85%, n=7). The behavioral accuracy of these three groups was significantly different (Figure 8B; one-way ANOVA: $F(2,18) = 44.39$, $p = 1.09 \times 10^{-7}$; Tukey's HSD: Early < Middle, $p = 6.2 \times 10^{-5}$; Middle < Late, $p = 0.0047$; Early < Late, $p = 7.31 \times 10^{-8}$).

Table 1. Task performance (percent correct) of each rat while recording the hippocampal neural activity during each session.

	Session1	Session2	Session3	Session4	Session5
Rat#1	64.7	78.5	83.5		
Rat#2	67.1	77.5	85.6		
Rat#3	62.3	66.4	83.3		
Rat#4	46.8	70.7	67.8	84.0	
Rat#5	56.1	63.6	78.0	88.6	
Rat#6	51.0	60.9	71.3	74.1	84.4
Rat#7	55.7	58.6	71.7	74.6	80.5

Table 2. The number of sessions required for each rat for recording of hippocampus to acquire the task.

	Rat#1	Rat#2	Rat#3	Rat#4	Rat#5	Rat#6	Rat#7
Pre-training	3	2	2	6	4	3	7
Learning	3	3	3	4	4	5	5

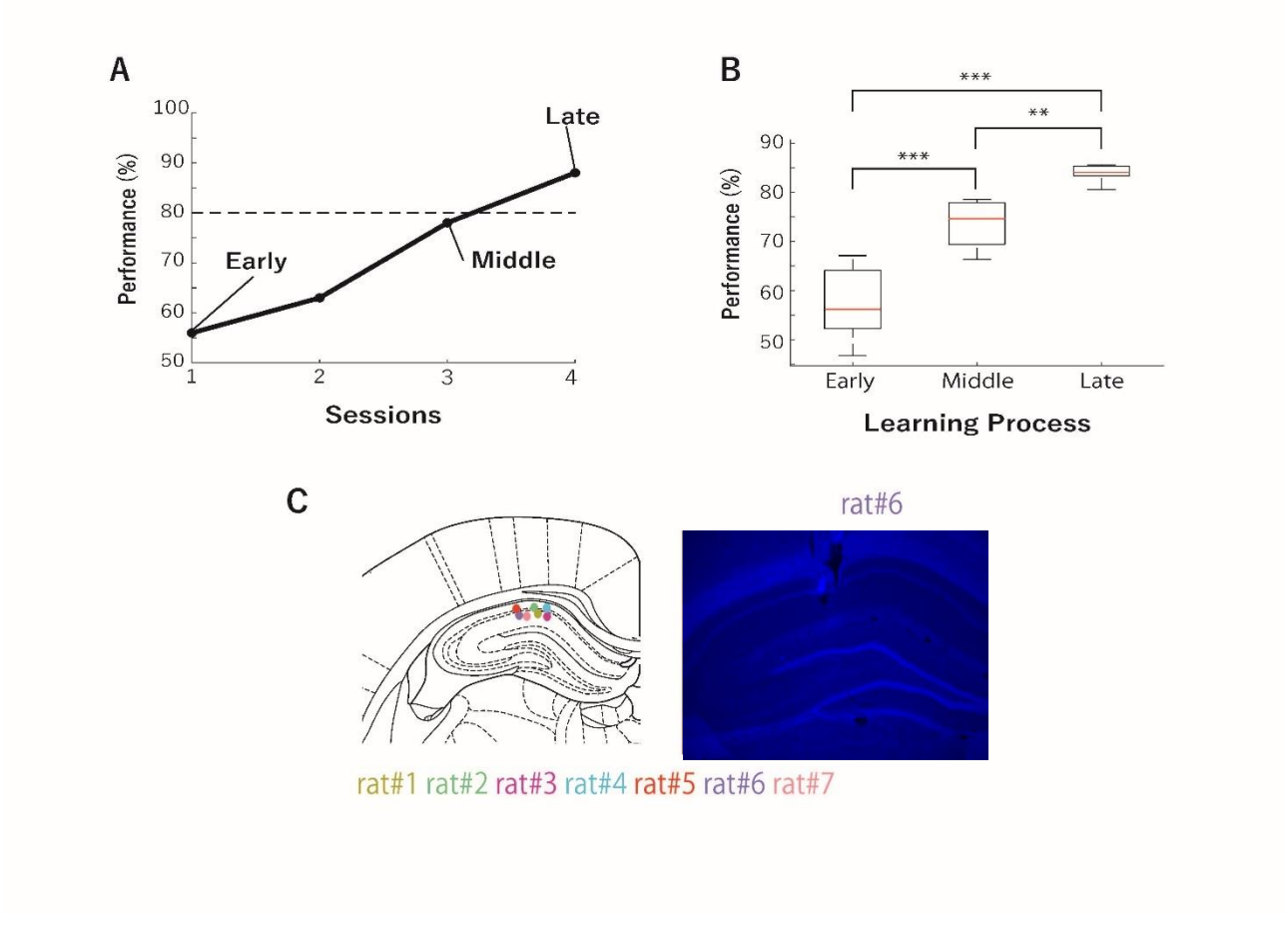

Figure 8. Behavioral performance and recording of neural activity in the hippocampal CA1.

(A) An example of performance in the associative memory task (rat #5). The dashed line indicates 80% correct. (B) Comparison of correct performance in early, middle, and late stages. in all rats (n = 7). Box limits show the 25th and 75th quartiles, and whiskers indicate maximum and minimum values. Median values are shown by red lines. (C) The coronal section was stained by DAPI, indicating recording sites in the hippocampal CA1. Each color dot corresponds to the animal identification number.

***$p < 0.01$; ** $p < 0.025$.

We recorded the spiking activity of 306 hippocampal CA1 cells from rats while they were learning the task (Figure 8C and Table 3). Neurons were categorized as putative pyramidal cells and interneurons based on their spike width (Figure 9A) (Isomura et al., 2009). We obtained 207 putative pyramidal neurons and 99 putative interneurons that showed significantly higher average firing rates than putative pyramidal neurons (Figure 9B: two-sample t-test, $p = 1.51 \times 10^{-8}$). In the early, middle, and late stages, 60, 63, and 47 putative pyramidal neurons were recorded, respectively. The tetrodes were not moved, and the constant-spike waveforms of the individual neurons were confirmed within a single session. The spike waveforms were also stable in repeated recordings on successive days. However, occasionally, some neurons disappeared, or new neurons appeared between recording sessions (Li et al., 2017), resulting in a variation in the number of recorded neurons among the three stages of learning.

Table 3. The number of pyramidal neurons (all neurons) in the hippocampal CA1 recorded in each rat during each session

	Session 1	Session 2	Session 3	Session 4	Session 5
Rat#1	4 (7)	15 (18)	13 (17)	-	-
Rat#2	14 (14)	18 (18)	13 (13)	-	-
Rat#3	15 (19)	3 (6)	5 (10)	-	-
Rat#4	4 (9)	4 (8)	8 (9)	2 (6)	-
Rat#5	7 (14)	5 (7)	3 (3)	1 (1)	-
Rat#6	7 (12)	10 (14)	7 (11)	10 (19)	8 (18)
Rat#7	9 (13)	6 (11)	5 (10)	6 (11)	5 (8)

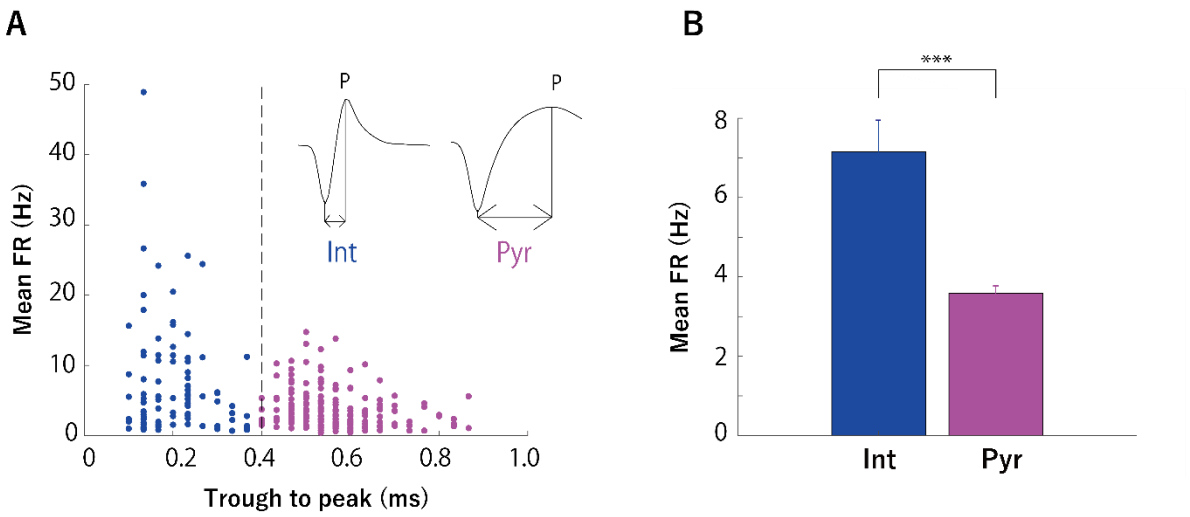

Figure 9. Cell classification.

(A) Classification of putative interneurons (Int, blue) and putative pyramidal neurons (Pyr, magenta) according to trough-to-peak width (dashed lines). Each spike waveform was classified by its width, which is calculated by subtracting the time at the troughs from that at the peak of each spike waveform (arrow lines). (B) Comparison of mean firing rates between putative pyramidal neurons (n = 207) and interneurons (n=99) (two-sample t-test; $p = 1.51\times10^{-8}$). Error bars indicate SEM. *** $p < 0.001$.

3.1.2 Choice-direction selective activity of CA1 pyramidal neurons

We observed that some pyramidal neurons showed choice-direction selective activity during the associative memory task (Figure 10A). These cells increased their firing rates in response to the choice of direction (left or right). The proportions of these cells were 48.3% (29 of 60), 42.9 % (27 of 63), and 36.2 % (17 of 47) in the early, middle, and late stages, respectively, without a significant difference among the learning stages (Figure 10B; chi-square test, χ^2 (2) = 1.59, n.s.). To assess the difference in the strength of selectivity among the learning stages, we calculated the degree of selectivity of each choice-direction cell based on their firing rates in the right- and left-choice trials. This value represents the difference between the firing rates of right-choice and those of left-choice by ratio. There were significant differences among the learning stages (Figure 10C; Kruskal–Wallis test, p = 0.021). The selectivity strength in the late stage was significantly lower than in the early stage (Wilcoxon rank sum test, $p = 7.7 \times 10^{-3}$).

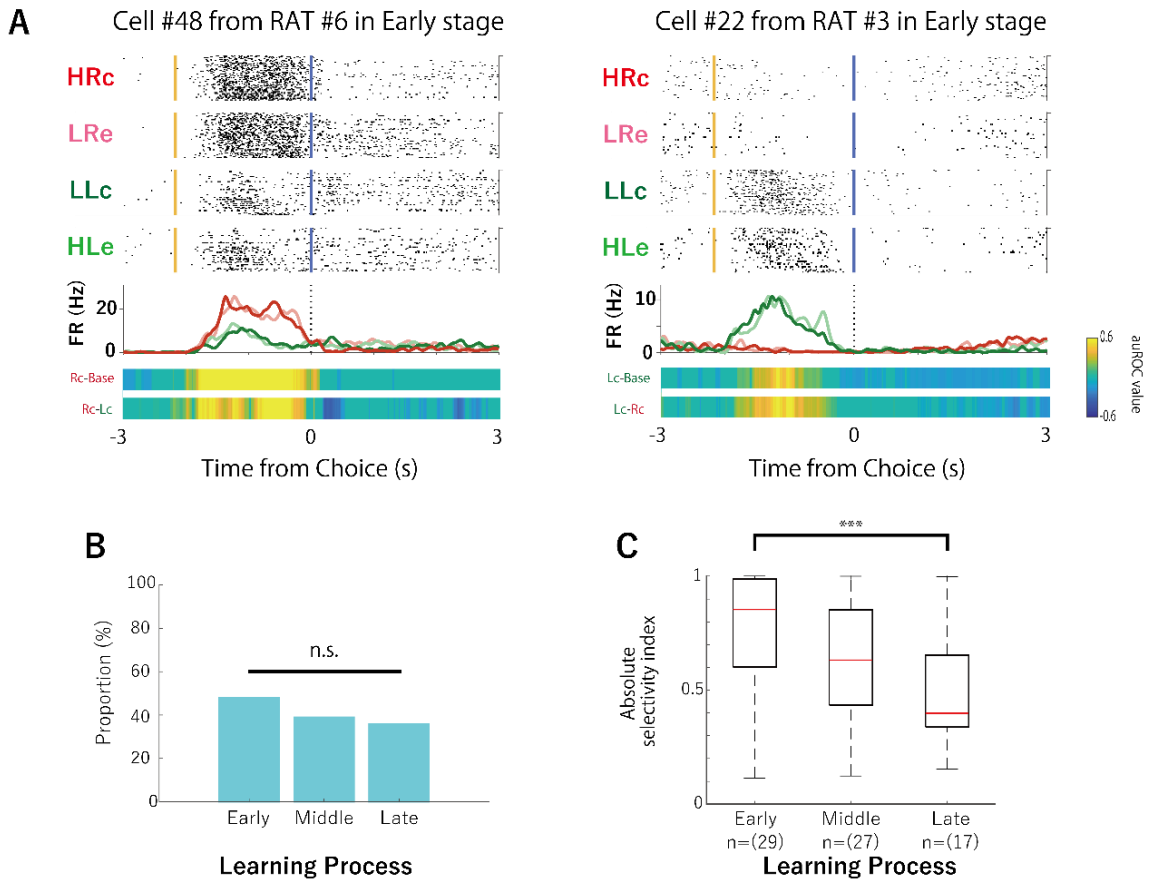

Figure 10. Proportion and selectivity of choice-direction cells in hippocampal CA1 during learning.

(A) Examples of the firing patterns of the choice-direction cells, which demonstrated firing modulation in right-choice trials (Cell # 48) and left-choice trials (Cell # 22). The data from 3 s before to 3 s after the choice is shown. Top panels: raster plots for each task condition; yellow and blue lines indicate the tone stimulus onset and choice response times, respectively. Middle panels: EASHs of HRc trials (red), LRe trials (pink), LLc trials (green), and HLe trials (light green). Dashed lines indicate the stimulus onset times. Bottom panels: auROC values of the task conditions for defining frequency-selective cells. The color scale represents the auROC values. (B) Comparison of the proportion of choice-direction cells among the learning stages. (C) Comparison of the selectivity of choice-direction selective cells among the learning stages. *** $p < 0.001$; n.s.: not significant, $p > 0.05$.

3.1.3 Reward-direction selective activity of CA1 pyramidal neurons

Some pyramidal neurons in CA1 showed reward-direction selectivity. Reward-direction cells increased their firing rates after the rats chose either of the correct ports (left or right) (Figure 11A). Therefore, the reward-direction cells consist of both right- and left-choice reward cells. The proportion of these cells differed significantly among the learning stages (Figure 11B; chi-squared test, $\chi 2\ (2) = 8.97$, $p < 0.025$). The proportions of these cells were 13.3 % (8 of 60) and 27 % (17 of 63) in the early and middle stages, respectively, but they showed a significant decrease to 6.4 % (3 of 47) in the late stage (Fisher's exact test with Holm correction; middle < late, $p = 0.017$). We then compared the strength of the reward-direction selectivity, but there were no significant differences among the learning stages (Figure 11C; Kruskal–Wallis test, $p = 0.79$).

We observed a few reward-direction cells that exhibited choice-direction selectivity. The proportion of these conjunctive cells was 5 % (3 of 60), 14.3 % (9 of 63), and 2.1 % (1 of 47) in the early, middle, and late stages, respectively. The proportion of these conjunctive cells differed significantly among the learning stages (chi-squared test, $\chi 2\ (2) = 6.55$, $p < 0.05$). The proportion of conjunctive cells in the middle stage was significantly higher than that in the late stage (Fisher's exact test with Holm correction; middle < late, $p = 0.041$).

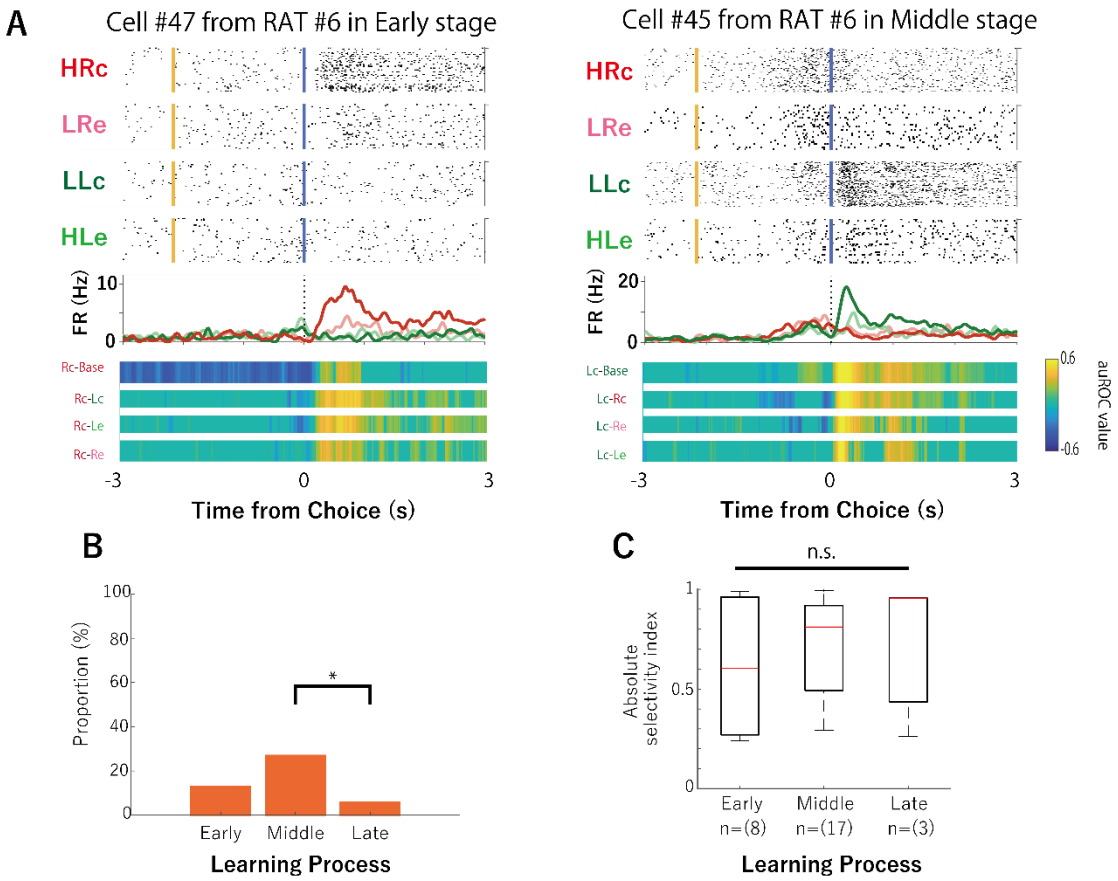

Figure 11. Proportion and selectivity of reward-direction selective cells in hippocampal CA1 during learning.

(A) Examples of the firing patterns of reward-direction selective cells, with firing increases in the HRc trials (Cell#47) and the LLc trials (Cell#45). The data from 3 s before to 3 s after the choice responses are shown. Top panels: raster plots for each task condition. Blue lines indicate the choice response times. Middle panels: EASHs of each task condition. Dashed lines indicate the choice response times. Bottom panels: auROC values of the task conditions for defining reward-direction selective cells. The color scale represents the auROC values. (B) Comparison of the proportion of reward-direction cells among the learning stages. (C) Comparison of the selectivity of choice-direction selective cells among the learning stages. Box limits show the 25th and 75th quartiles, and whiskers indicate maximum and minimum values. Mean values are shown by red lines. * $p < 0.05$. n.s.: not significant, $p > 0.05$.

Table 4. Numbers of task-related cells and conjunctive cells in the hippocampal CA1 during each learning stage

	Early	Middle	Late
Choice-direction cells	26	18	16
Reward-direction cells	5	8	2
Conjunctive cells	3	9	1

3.2 Auditory cortex neurons show task-related and learning-dependent activity

3.2.1 Learning of the associative memory task and recording of neural activity from A1

We next recorded and analyzed the neural activity of the A1 during the learning process of the same task because modulations of neural activity in hippocampal CA1 might influence A1 neurons, which play a role in processing tone discrimination. Six rats were trained in the associative memory task with frequencies of 3 kHz and 1 kHz as pre-training. The rats performed the task in two to eight sessions (days) (Table 6). The electrodes were implanted when the rats completed the pre-training. A week after the surgery for electrode implantation, the rats began to learn the task at frequencies of 10 kHz and 6 kHz (learning sessions). The rats performed the task in 3–5 sessions (i.e., 3–5 days). Table 5 shows the percentage of correct responses from each animal during each session. Figure 12A shows examples of the task performance of three rats: one was a fast learner (rat #1), and the others were slow learners (rats #3 and #6) that showed different learning curves. We divided the learning sessions into three stages. The first session was defined as the "early-stage" (mean behavioral accuracy = 59.80 %, n = 6), the last session as the "late-stage" (mean behavioral accuracy = 84.41 %, n = 6), and the sessions before the last session as the "middle-stage" (mean behavioral accuracy = 74.49 %, n = 6). The middle stage could be the second, third, or fourth session, and the last stage could be the third, fourth, or fifth session, according to the performance of

each animal. The behavioral accuracy of these three stages differed significantly (Figure 12B; one-way analysis of variance [ANOVA]: $F(2,15) = 32.18$, $p = 3.75 \times 10^{-6}$; Tukey's HSD: early < middle, $p = 6.98 \times 10^{-4}$; middle < late, $p = 0.02$; and early < late, $p = 2.56 \times 10^{-6}$). The rats' performance gradually increased during the first, second, and last stages. This gradual increase became apparent when the total number of learning sessions was divided into three stages according to the task performance of each animal. We also compared the accuracy of the first (early stage), second (mean behavioral accuracy = 69.54 %, n = 6), and third sessions (mean behavioral accuracy = 72.90 %, n = 6), but the differences were not significant (Figure 12C; one-way ANOVA: $F(2,15) = 2.83$, $p = 0.09$). We compared the performance of these sessions to reveal that the differences in neuronal activity depend on increases in task performance (learning) and session numbers (trials). Although task performance seemed to increase gradually during the first, second, and third sessions (Figure 12C), the increase was not statistically significant due to the high variability in each session. However, as described above, the increase in task performance during the early, middle, and late stages was highly significant (Figure 12B).

Table 5. Task performance (percent correct) of each rat during the recording of neural activity in the A1 in each session.

	Session 1	Session 2	Session 3	Session 4	Session 5
Rat#1	58.1	65.4	82.3	-	-
Rat#2	70.7	78.2	80.4	-	-
Rat#3	65.1	76.7	71.3	72.6	84.7
Rat#4	49.7	59.5	53.2	77.1	84.2
Rat#5	59.9	78.2	86.8	-	-
Rat#6	55.3	59.0	64.0	75.4	88.0

Table 6. The number of sessions required for each rat for recording of A1 to acquire the task.

	Rat#1	Rat#2	Rat#3	Rat#4	Rat#5	Rat#6
Pre-training	2	2	6	8	5	4
Learning	3	3	5	5	3	5

We recorded the spiking activity of the A1 cells of the rats when they were learning the task (Figure 12D and Table 7). We recorded 66, 52, and 44 neurons in the early, middle, and late stages, respectively, and 66, 63, and 49 neurons in the first (early), second, and third sessions, respectively. The tetrodes were not moved, and the constant-spike waveforms of the individual neurons were confirmed within a single session. The spike waveforms were also stable in repeated recordings on successive days (Figure 12E). The waveform consistency also indicates consistency among the neuron types (pyramidal neurons vs. interneurons) throughout the learning stages, as pyramidal neurons and interneurons have different spike waveforms. These results suggested that the recordings were most likely from the same cell population. However, occasionally, some neurons disappeared, or new neurons appeared between recording sessions (Li et al., 2017), resulting in a variation in the number of recorded neurons among the three stages of learning.

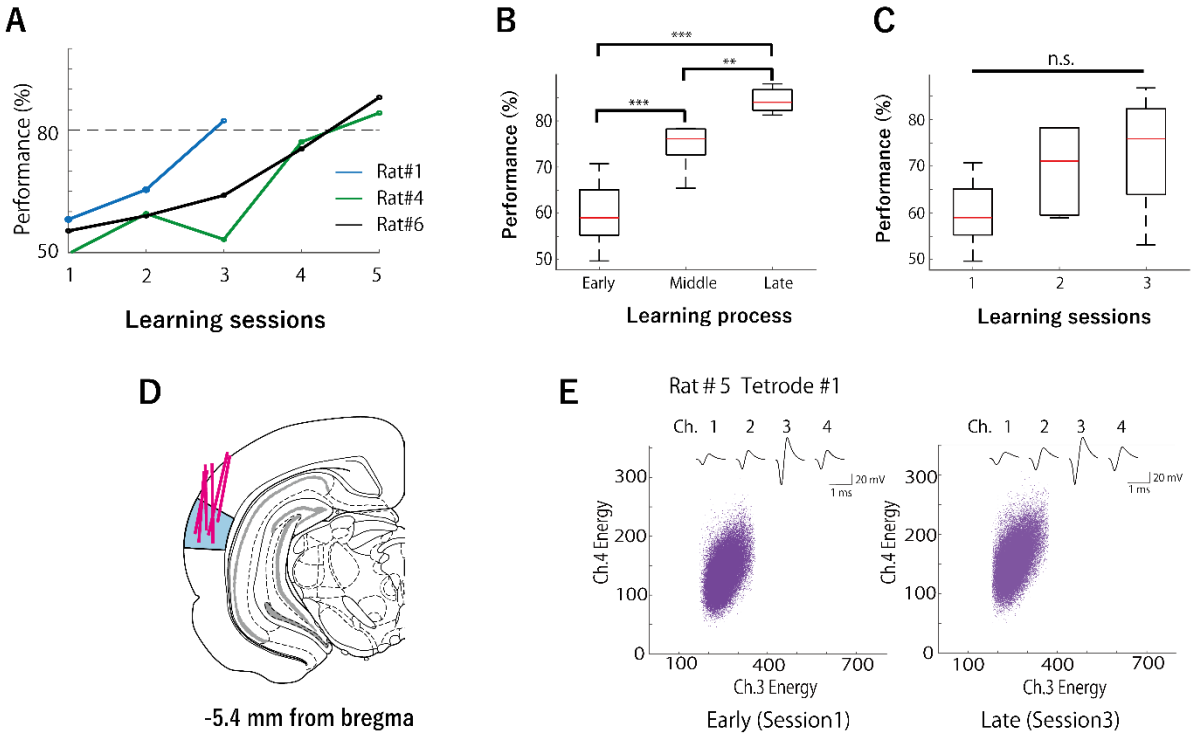

Figure 12. Task performance and recording of neural activity in A1.

(A) Examples of performance in the associative memory task (rats #1, #4, and #6). (B) Comparison of correct task performance during each learning stage in all rats (n = 6). Box limits show the 25th and 75th quartiles, and whiskers indicate maximum and minimum values. Median values are shown by red lines. (C) Comparison of correct task performance in the first, second, and third sessions in all rats (n = 6). (D) Coronal section view showing the recording sites in the primary auditory cortex (blue). Red lines indicate the track of the movable tetrodes. (E) An example of spike waveform consistency is during the early (left) and late (right) stages. Top: the averaged spike waveforms on each channel of tetrode #1. Bottom: Scatter plots of the spike clusters during the early (left) and late (right) stages. Each purple point represents a spike. The horizontal and vertical axes represent the energy of the spikes as detected by channels 3 and 4 of tetrode #1, respectively.

***$p < 0.01$; ** $p < 0.025$; n.s.: not significant, $p > 0.05$.

Table 7. Number of neurons in the A1 recorded in each rat during each session.

	Session 1	Session 2	Session 3	Session 4	Session 5
Rat#1	16	13	7	-	-
Rat#2	5	7	8	-	-
Rat#3	4	4	2	2	2
Rat#4	14	16	10	10	10
Rat#5	8	8	8	-	-
Rat#6	19	15	14	12	9

3.2.2 Frequency-selective activity of A1 neurons

We observed frequency-selective cells that increased or decreased their firing rates in response to tonal differences (high or low), regardless of whether the choice was left or right and correct or incorrect (Figure 13A). These frequency-selective cells were observed in each session, but their proportions differed significantly among learning stages (Figure 13B; chi-square test, $\chi 2\ (2) = 16.38$, $p < 0.01$). We observed that 21.2 % (14 of 66) of the neurons had frequency selectivity in the early stage, and the proportion of the neurons significantly increased to 59.1 % (26 of 44 neurons) in the late stage (Fisher's exact test with Holm correction; early < late, $p = 9.43 \times 10^{-5}$). However, frequency selectivity was observed only in 22 % (14 of 63) and 34 % (17 of 49) of the neurons in the second and third sessions, respectively, without significant differences among the first, second, and third sessions (Figure 13C; chi-square test, $\chi 2\ (2) = 3.18$, n.s.).

To assess the difference in the strength of selectivity among the learning stages, we calculated the degree of selectivity of each of the frequency-selective cells based on their firing rates in the high-tone and low-tone trials. There were no significant differences among the learning stages (Figure 13D; Kruskal–Wallis test, $p = 0.17$) or among the first, second, and third sessions (Figure 13E; Kruskal–Wallis test, $p = 0.21$).

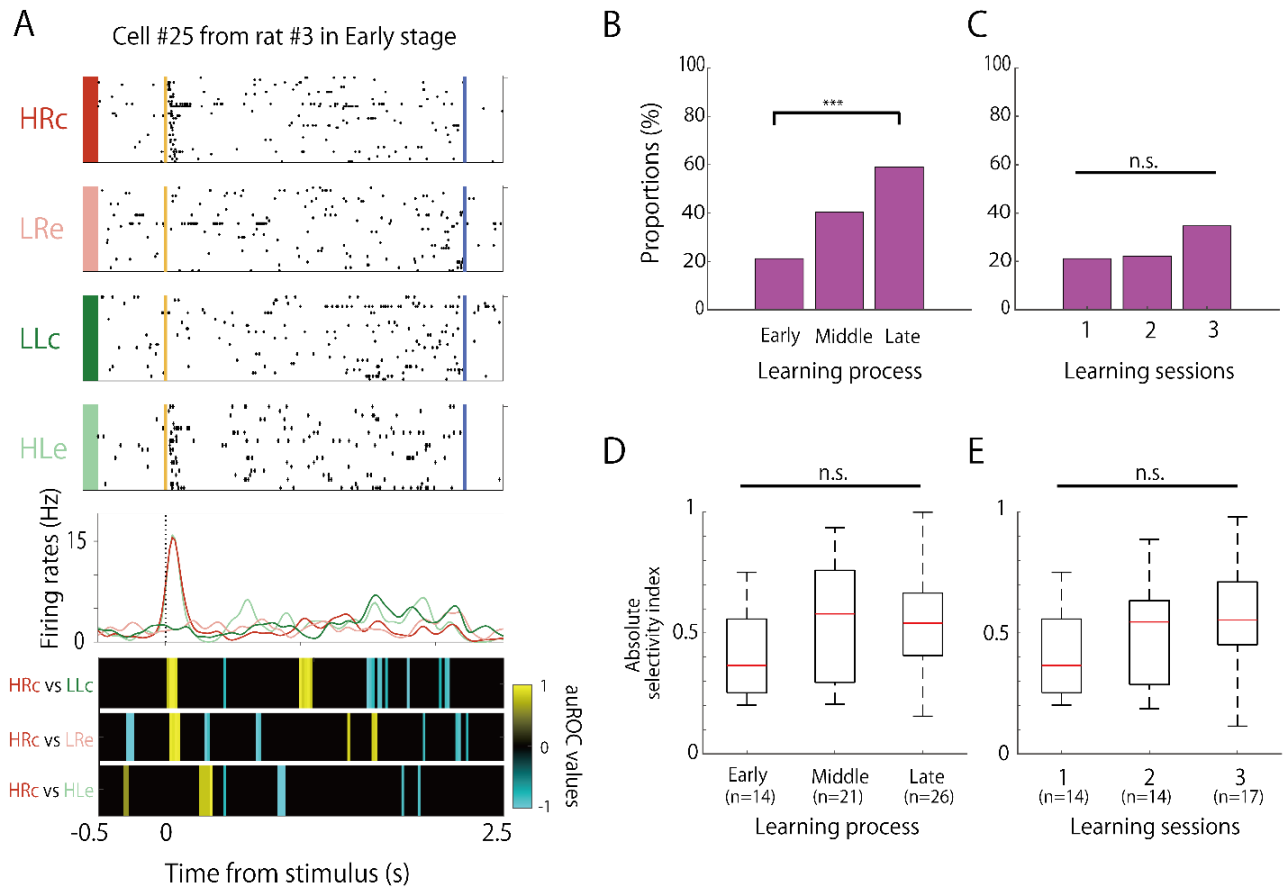

Figure 13. Proportion and selectivity of frequency-selective cells in A1 during learning.

(A) An example of the firing patterns of the frequency-selective cells, which demonstrated firing modulation in high tone trials. The data from 0.5 s before to 2.5 s after stimulus onset are shown. Top panels: raster plots for each task condition; yellow and blue lines indicate the tone stimulus onset and choice response times, respectively. Middle panels: EASHs of HRc trials (red), LRe trials (pink), LLc trials (green), and HLe trials (light green). Dashed lines indicate the stimulus onset times. Bottom panels: auROC values of the task conditions for defining frequency-selective cells. The color scale represents the auROC values. Nonsignificant auROC values close to 0 are expressed in black. (B) Comparison of the proportion of frequency-selective cells among the learning stages. (C) Comparison of the proportion of frequency-selective cells among the learning sessions. (D) Comparison of the selectivity of frequency-selective cells among the learning stages. Box limits show the 25th and 75th quartiles, and whiskers indicate maximum and minimum values. Median values are shown by red lines. (E) Comparison of the selectivity of frequency-selective cells among the learning sessions. ***$p < 0.01$; n.s.: not significant, $p > 0.05$

3.2.3 Frequency-selective activity engagement in the task

To investigate whether the frequency selectivity of A1 cells was engaged in the task, we compared the firing activity between the associative memory task (27 cells) and the passive tone condition (32 cells) in three of the six rats. The tetrodes were not moved, and the recorded cells were from the same cell populations as those used in the task training. In the passive tone condition, 25% (8 of 32) of the neurons showed sound-evoked firing that was modulated by tone presentation, regardless of the tone frequency (Figure 14A). This type of frequency-insensitive firing was not observed in the associative memory task (Figure 14B). Moreover, 44% (12 of 27) and 19 % (6 of 32) of the neurons were frequency-selective cells (e.g., Figure 13) in the task and passive tone conditions, respectively. The proportion of frequency-selective cells was significantly higher in the task than in the passive tone condition (Figure 14C; Fisher's exact test, $p = 4.75 \times 10^{-2}$). Furthermore, the frequency selectivity of the frequency-selective cells was higher in the task than in the passive tone condition (Figure 14D; Wilcoxon rank sum test, $p = 7.54 \times 10^{-4}$).

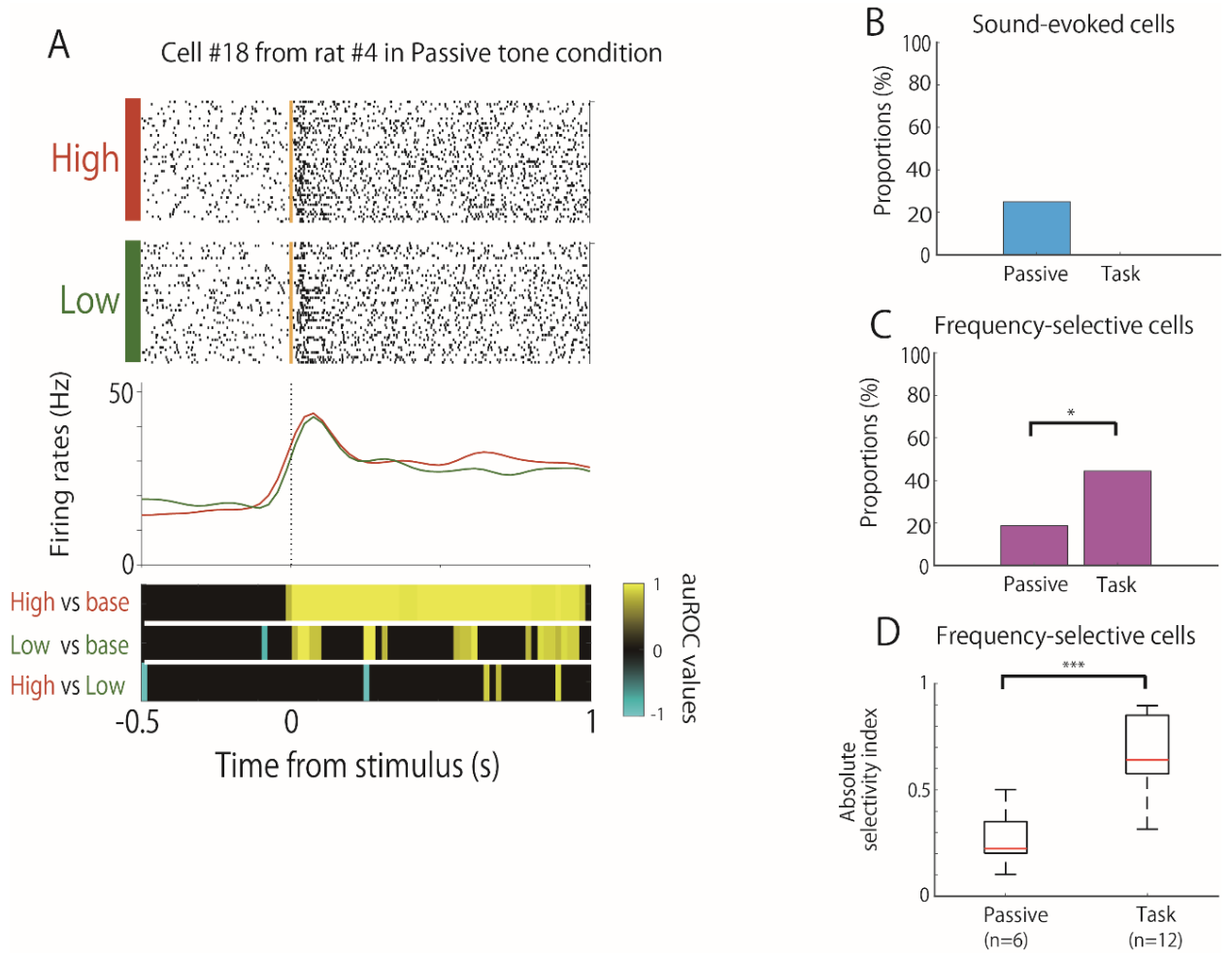

Figure 14. Comparison of the neural activity between the task and passive tone condition.

(A) An example of the firing patterns from sound-evoked cells, which demonstrated firing increases during stimulus onset. The data from 0.5 s before to 1 s after stimulus onset are shown. Top panels: Raster plots for each tone condition. Yellow lines indicate the stimulus tone onset times. Middle panels: PSTHs of high-tone and low-tone trials (red) and low-tone trials (green). Dashed lines indicate the stimulus onset times. Bottom panels: auROC values of the task conditions for defining sound-evoked cells. The color scale represents the auROC values. Nonsignificant auROC values close to 0 are expressed in black. (B) Comparison of the proportion of sound-evoked cells between the task and passive tone conditions. (C) Comparison of the proportion of frequency-selective cells between the task and passive tone conditions. (D) Comparison of the selectivity of frequency-selective cells between the task and passive tone condition. Box limits show the 25th and 75th quartiles, and whiskers indicate maximum and minimum values. Median values are shown by red lines.

***$p < 0.01$; *$p < 0.05$; n.s.: not significant, $p > 0.05$.

3.2.4 Choice-direction selective activity of A1 neurons

We observed choice-direction-selective cells during the associative memory task. These cells modulated their firing rates in response to the choice of direction (left or right), regardless of whether the tone was high or low and whether the choice was correct or incorrect (Figure 15A). The proportions of these cells were 9 % (6 of 66), 19 % (10 of 52), and 18 % (8 of 44) in the early, middle, and late stages, respectively, without a significant difference among the learning stages (Figure 15B; chi-square test, $\chi 2$ (2) = 2.91, n.s.). The proportion of the choice-direction selective cells in the second and third sessions was 12.7 % (8 of 63) and 10.2 % (5 of 49), respectively, but there were no significant differences among them (Figure 15C; chi-square test, $\chi 2$ (2) = 0.46, n.s.). We then compared the strength of the choice-direction selectivity, but there were no significant differences among the learning stages (Figure 15D; Kruskal–Wallis test, $p = 0.42$) or the three sessions (Figure 15E; Kruskal–Wallis test, $p = 0.54$).

We also observed several choice-direction cells that exhibited frequency selectivity (Table 8). The proportion of these conjunctive cells was 1.5 % (1 of 66), 3.8 % (2 of 52), and 9.1 % (4 of 44) in the early, middle, and late stages, respectively.

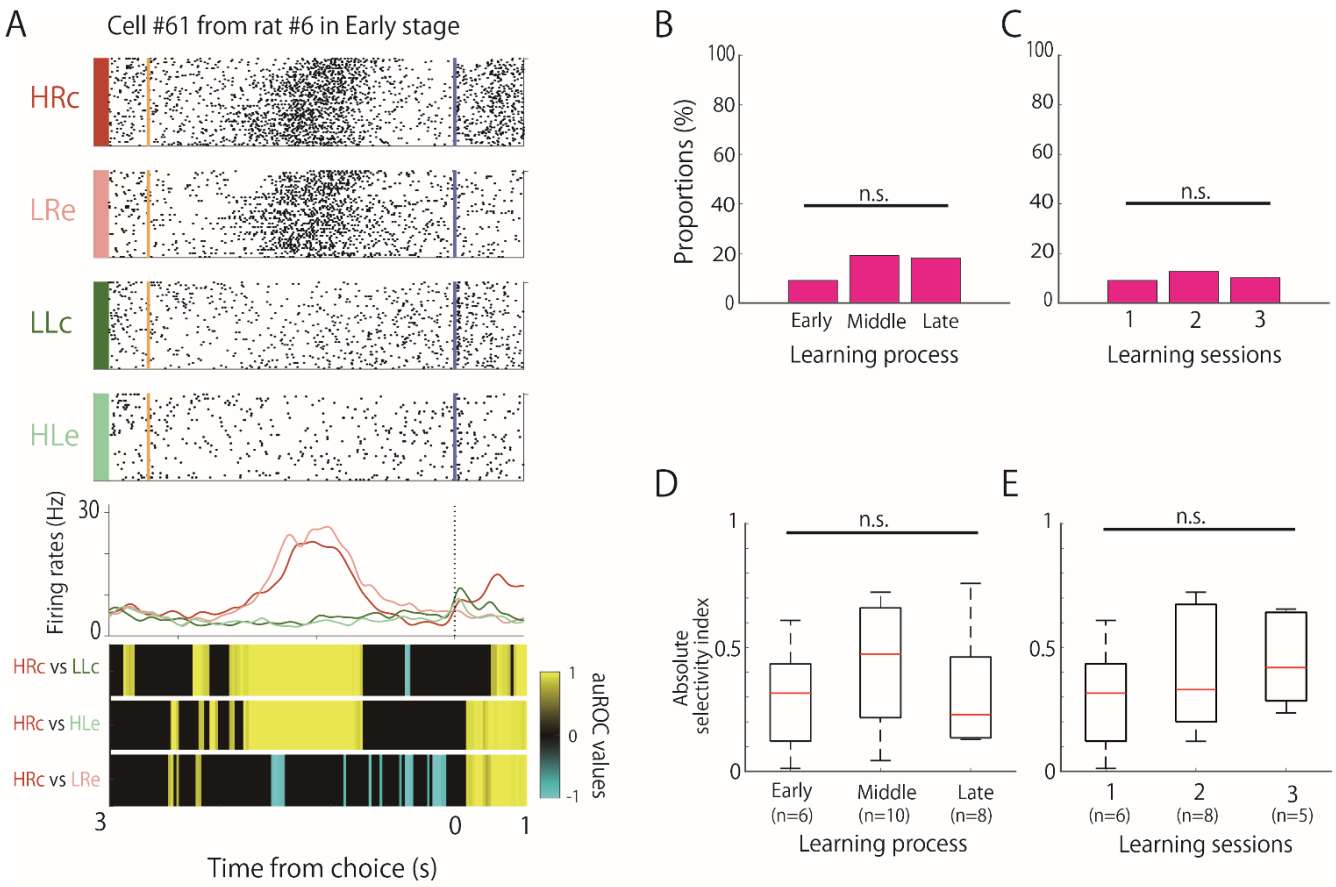

Figure 15. Proportion and selectivity of choice-direction selective cells in A1 during learning.

(A) An example of the firing patterns of choice-direction selective cells, with firing increases in the right choice trials presented. The data from 3 s before to 1 s after the choice responses are shown. Top panels: raster plots for each task condition; yellow and blue lines indicate the tone stimulus onset and choice response times, respectively. Middle panels: EASHs of each task condition. Dashed lines indicate the choice response times. Bottom panels: auROC values of the task conditions for defining choice-direction selective cells. The color scale represents the auROC values. Nonsignificant auROC values around or close to 0 are expressed in black. (B) Comparison of the proportion of choice-direction selective cells among the learning stages. (C) Comparison of the proportion of choice-direction selective cells among the learning sessions. (D) Comparison of the selectivity of choice-direction selective cells among the learning stages. Box limits show the 25th and 75th quartiles, and whiskers indicate maximum and minimum values. Median values are shown by red lines. (E) Comparison of the selectivity of choice-direction selective cells among the learning sessions. n.s.: not significant, $p > 0.05$.

3.2.5 Reward-direction selective activity of A1 neurons

Some neurons in A1 showed reward-direction selectivity. Reward direction-selective cells modulated their firing rates after the rats chose either of the correct ports (left or right) (Figure 16A). Therefore, the reward-direction cells consist of both right- and left-choice reward cells.

As shown in Figure 16A, there were distinct effects on the immediate phasic response following reward delivery after choosing the left port (LLc). However, there was no significant difference in the phasic response between LLc and HRc, as shown by the auROC values at the bottom of Figure 16A. Therefore, the phasic response of this neuron did not exhibit directional selectivity. The auROC values also showed that the prolonged responses that followed the reward delivery after choosing the right port (HRc) contributed to the directional selectivity of this neuron.

Concerning the dichotomy between the early (phasic) and late (prolonged) responses, we analyzed the activity of each reward-direction cell in the phasic and prolonged periods separately. We observed that 10% of the reward-direction cells (2 of 20) showed both phasic and sensory responses after the reward buzzer and prolonged responses corresponding to reward and choice of direction. The other reward-direction cells showed only a prolonged response corresponding to the reward and choice of directions.

The proportion of these cells differed significantly among the learning stages (Figure

16B; chi-squared test, $\chi 2$ (2) = 8.46, $p < 0.025$). The proportions of these cells were 4.5 % (3 of 66) and 3.8 % (2 of 52) in the early and middle stages, respectively, but they showed a significant increase to 18 % (8 of 44) in the late stage (Fisher's exact test with Holm correction; middle < late, $p = 0.04$). However, in the second and third sessions, the proportions of these cells were 3.2 % (2 of 63) and 10.2 % (5 of 49), respectively, without significant differences among the three sessions (Figure 16C; chi-square test, $\chi 2$ (2) = 2.80, n.s.).

We observed a few reward-direction cells that exhibited frequency selectivity (Table 8). The proportion of these conjunctive cells was 1.5 % (1 of 66), 1.9 % (1 of 52), and 9.1 % (4 of 44) in the early, middle, and late stages, respectively. We also observed a few reward-direction cells that exhibited choice-direction selectivity. The proportion of these conjunctive cells was 1.5 % (1 of 66), 1.9 % (1 of 52), and 6.8 % (3 of 44) in the early, middle, and late stages, respectively.

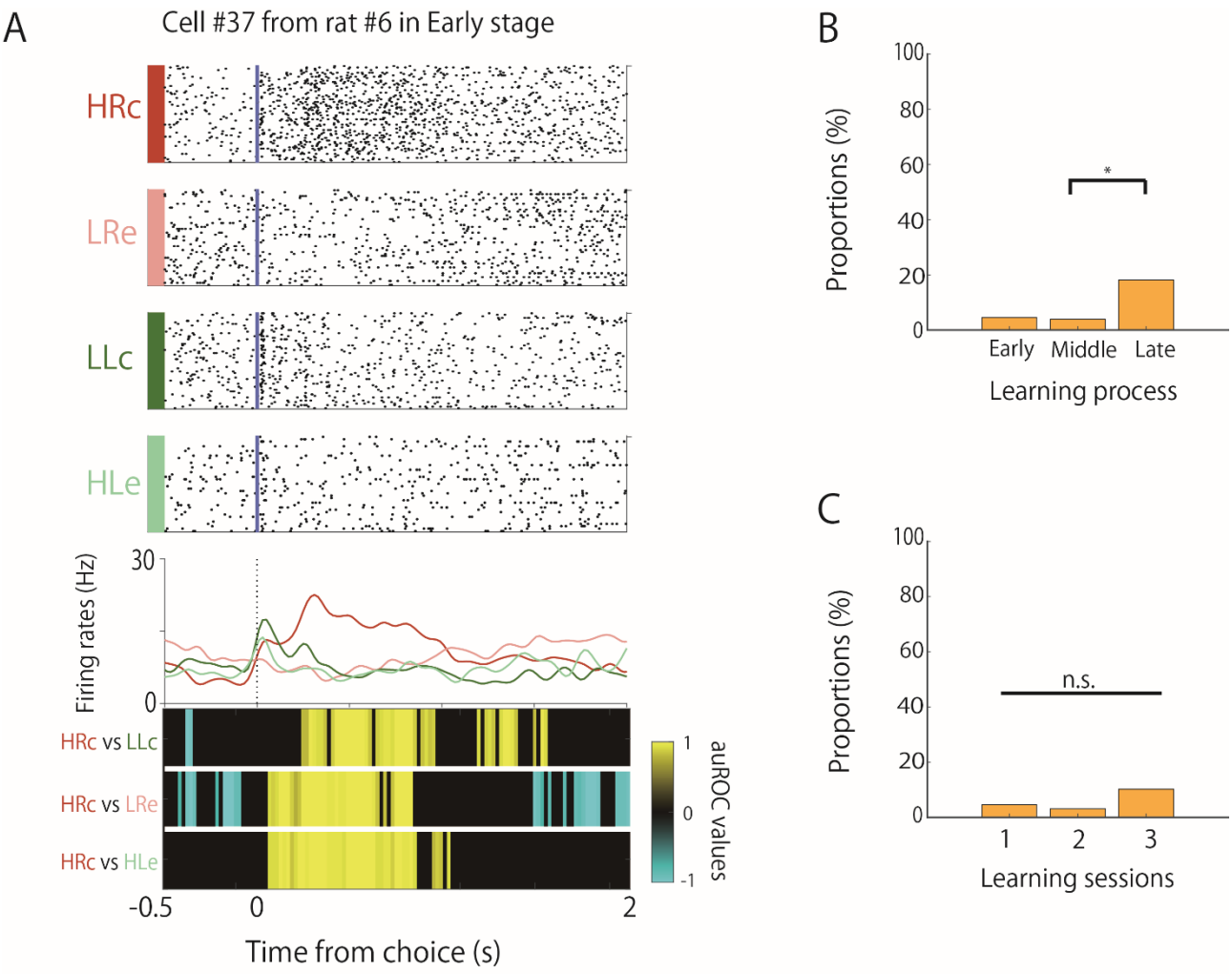

Figure 16. Proportion of reward-direction selective cells in A1 during learning.

(A) An example of the firing patterns of reward-direction selective cells, with firing increases in the HRc trials presented. The data from 0.5 s before to 2 s after the choice responses are shown. Top panels: raster plots for each task condition. Blue lines indicate the choice response times. Middle panels: PSTHs of each task condition. Dashed lines indicate the choice response times. Bottom panels: auROC values of the task conditions for defining reward-direction selective cells. The color scale represents the auROC values. Nonsignificant auROC values close to 0 are expressed in black. (B) Comparison of the proportion of reward-direction selective cells among the learning stages. (C) Comparison of the proportion of reward-direction selective cells among the learning sessions. *$p < 0.05$; n.s.: not significant, $p > 0.05$.

Table 8. Numbers of task-related cells and conjunctive cells in the A1 in each learning stage

	Early	Middle	Late
Frequency selective cells	12	18	18
Choice-direction cells	4	7	1
Reward-direction cells	1	0	1
Conjunctive cells			
Frequency & Choice-direction	1	2	4
Frequency & Reward-direction	1	1	4
Choice & Reward-direction	1	1	3

Chapter 4 Discussion

4.1 Hippocampal CA1 neurons represent positive feedback during the learning process

In this experiment assessing the hippocampal CA1, we report the neuronal activity during the entire process of learning an auditory associative memory task. We found that several pyramidal neurons showed choice-direction selective (Figure 10A) or reward-direction selective activity (Figure 11A). Our results suggest that each hippocampal CA1 neuron represents each event of the task and contributes to forming associative memory. The property of choice-direction cells might be the association between cue tone and choice (Terada et al., 2017) or goal-directed encoding (Aoki et al., 2019; Igata et al., 2020). Terada et al. (2017) showed hippocampal CA1 neurons respond to cue tones and/or choice of directions, and Aoki et al. (2019) and Igata et al. (2020) showed firing rates of CA1 neurons increased when animals reached the goal location where they could obtain rewards. However, the proportion of the choice-direction cells was not learning-dependent. It did not significantly differ among the learning stages (Figure 10B), suggesting that these cells might not depend on associative memory formation and consolidation. Their firing might reflect a stable function in hippocampal CA1 throughout the learning process, such as spatial coding of choice and/or ports.

For the reward-direction cells, we observed that their proportion was learning-dependent (Figure 11B) and significantly decreased in the late stage of the learning

process, although the rats received the highest amount of reward at the last stage. It is obvious that the reward-direction cells do not represent reward delivery itself because of their learning-dependent property. Previous studies have revealed that some hippocampal neurons represent reward-predicted encoding and called such neurons "reward cells" (Gauthier and Tank, 2018). However, in our study, reward-direction cells did not represent reward-predicted encoding or reward locations because these cells were activated after the rats chose the correct port and the reward buzzer was presented, and reward pellets were delivered into the same location (pellet magazine in Figure 5) irrespective of the location of the correct port. Therefore, the firing of reward-direction cells might reflect "positive feedback" of the correct port choice to form the association of auditory stimuli and port directions. They play a role in reinforcement learning only when the learning is not completely acquired, and their proportion significantly decreases in the late stages of learning (Figure 11B). In reinforcement learning, positive feedback is crucial to enable understanding of tasks, and it is important in the middle stage of the learning process (Maia, 2009; Littman, 2015). Thus, the reward-direction cells in the CA1 might underlie the positive feedback required for learning progress. However, after the completion of learning, the activation of these CA1 cells might become unnecessary as learned information is transferred to the neocortex for memory consolidation.

Although it is unclear whether associative memory and reinforcement learning rely on a common neural substrate in the hippocampus, it may be useful to discuss the present data of reward-direction cells from a reinforcement learning perspective, e.g., the idea of the successor representation (SR) (Stachenfeld et al., 2017; Gershman, 2018). Besides that, the SR is closely related to place fields observed in the hippocampal CA1 (Stachenfeld et al., 2017); it takes on richer characteristics in other complex environments. If the hippocampus encodes the SR, we can predict how it will respond to transition and reward manipulations in revaluation experiments (Momennejad et al., 2017). What seems to be examined, particularly in relation to the positive-feedback signals of the reward-direction cells, is whether the cells convey vector-valued signals to update the SR (Gershman, 2018). Ensemble recordings of reward-related cells will be useful in answering this question.

The reward-direction cells that have a joint feature of reward state and direction seem to be relevant to the multidimensional features of the hippocampal neurons (Nieh et al. 2021). Nieh et al. (2021) examined how neurons in the CA1 integrated neural representations of cognitive and physical variables and whether low-dimensional manifolds underlie these representations. They found that most task-related neurons encoded position and evidence jointly in the multidimensional spaces and suggested that the neural encoding of the task variables at the cellular level may have a geometric

structure.

Since the pioneering study by James Olds and his colleagues (e.g., Olds et al., 1972), many studies have investigated neural activity changes during learning processes (e.g., McEchron and Disterhoft, 1997; Wirth et al., 2003, Igarashi et al., 2014; Modi et al., 2014). McEchron et al. (1997) reported that CA1 pyramidal neurons demonstrated changes in activity after the CS and/or US in different learning stages of trace eyeblink conditioning. Modi et al. (2014) found that CA1 neurons transiently increased their spontaneous activity correlations during trace eyeblink conditioning, and the correlated neurons fell into distinct spatial clusters that changed CA1 as a result of learning. Wirth et al. (2003) reported that hippocampal neurons signaled the acquisition of new associations by changing their stimulus-selective response properties. Igarashi et al. (2014) identified the entorhinal–hippocampal coupling by 20–40-Hz oscillations as a key mechanism for the formation and retrieval of associative memory.

These previous studies reported cue-evoked firing patterns and associated changes in hippocampal CA1 neurons with learning and have yielded extensive information about their role in learning. In contrast, the present study shows learning-related changes in reward-evoked activity. We demonstrated an increment in the activity of reward-direction cells in the CA1 during the middle stage of learning. Therefore, the present study might further reveal the role of hippocampal CA1 neurons in learning associative

memory by suggesting that CA1 pyramidal neurons are working to provide the animal with positive feedback regarding the correct association to acquire associative memory.

4.2 Auditory cortex neurons show learning-dependent selectivity toward not only sound input but also rewards

In this study for A1, we examined neuronal activity during the entire process of learning an auditory associative memory task, as we did for hippocampal CA1. We found that A1 neurons showed selectivity for tone frequencies, choice of directions, and reward directions. The proportion of frequency-selective and reward-direction cells increased during task acquisition. Therefore, A1 neurons showed learning-dependent modulation of activity when associations between auditory tones and behavioral responses were gradually induced by learning.

The proportion of frequency-selective cells was learning-dependent and increased significantly in the late stages of the learning process (Figure 13B). This increase in the proportion was not caused by a simple increase in sessions but by a significant increase in correct performance due to learning. This conclusion was derived because the proportion of cells did not differ significantly among the first, second, and third sessions, wherein the correct performance on the task did not increase (Figure 13C). Furthermore, the selectivity was not due to the difference between the correct and incorrect trials.

This is because the auROC values of the HRc vs. HLe and LLc vs. LRe conditions were not significant in high-frequency selective cells and low-frequency selective cells, respectively. These comparisons indicated that the activity of the frequency-selective cells was modulated only by frequency and not by correct or erroneous trials. The strength of selectivity in these cells, however, did not differ significantly among the learning stages and sessions (Figures 13D and 13E). The strength of the selectivity had to increase for each cell to become frequency selective. However, learning dependency was related to the increase in the number of frequency-selective cells and not to the increase in the strength of each selective cell. These results suggest that tone frequency selectivity in A1 increases during the learning process by increasing the frequency-selective cells but not by increasing the strength of the frequency selectivity of each cell. This modulation of proportions might be related to plastic changes in the tonotopic map related to the learning task, as the tetrodes were not moved throughout the successive days of training and the recording sites were not changed. The proportion of frequency-selective cells was also significantly different between the task and passive tone conditions (Figure 14C), and the strength of the selectivity was significantly higher in the former than in the latter (Figure 14D). Furthermore, some frequency-selective cells showed phasic modulation in brief periods following tone presentation, whereas others showed tonic modulation during tone presentation. These results suggest that the

frequency selectivity of A1 neurons emerges strongly when the tone is also involved in a task with choices and rewards.

Some previous studies reported that the representation area of tone frequency in the A1 increased with learning (Recanzone et al., 1993; Polley et al., 2006), and enlargement occurred very quickly in several trials (Edeline and Weinberger, 1993; Fritz et al., 2003, 2005). However, in our results, the number of frequency-selective cells increased over a longer time span of several days. This might be due to the differences in the demands and difficulties of the tasks between previous studies and this study. In other words, the conditions may have been simpler in the former than in the latter, which could have been responsible for the slow progress. This notion is supported by previous studies reporting that the sound-evoked activity of A1 neurons is modulated by task engagement (De Franceschi and Barkat, 2021; Atiani et al., 2009) and task structures (David et al., 2012).

A1 neurons also showed choice-direction selectivity, and the proportion of these cells did not differ significantly among learning stages (Figure 15B). These cells might not be affected by the different acoustic properties of the different parts of the experimental chamber, as the distance between the right and left ports was only 70 mm and the distance from the loudspeaker was 550 mm for both ports. Furthermore, the selectivity of the choice-direction cells was not affected by the difference between the correct and

erroneous trials. This is because the auROC values of the HRc vs. LRe and LLc vs. HLe conditions were not significant for right- and left-choice selective cells, respectively. This indicates that A1 neurons represent tone signals and behavioral choice information, and these representations are stable throughout the learning process.

The activity of A1 neurons in response to behavioral movements has been reported in previous studies (Nelson et al., 2013; Rummell et al., 2016). In addition, Guo et al. (2019) reported that A1 and posterior striatum neurons show choice-direction selectivity based on reward expectations. Choice-related activity has also been found in other parts of the primary sensory cortex, such as the visual cortex (Stringer et al., 2021) and the olfactory cortex (Miura et al., 2012; Poo et al., 2021). These responses in previous studies were not necessarily associated with the formation of associations that led to the consolidation of associative memory. Therefore, it could be suggested that choice of directions in associative learning are represented in several brain regions, including the sensory cortex and hippocampus, and that such representations have stable functions throughout the learning process.

We found that some A1 neurons showed reward-direction selectivity, and the proportion of reward-direction selectivity in the late stage of the learning process was significantly higher than that in the early stage (Figure 16B). This suggests that A1 neurons represent reward directions, tone frequencies, and choice directions, and the

proportion of these cells increased when the rats learned the associative memory task. The increases in the reward-direction cells did not depend on the number of sessions but on the accuracy of the task. This conclusion was drawn because the proportion of these cells did not significantly differ among the first, second, and third sessions, wherein there was no improvement in accuracy (Figure 16C). The activity of the reward-direction cells was not affected by the buzzer sounds related to reward delivery nor by sounds from the food delivery system or motor aspects of reward consumption, as these sounds were present in both the right- and left-choice reward trials. If these sounds from rewarded trials affected neuronal activity, the neurons should have shown the same firing rate modulations in both the right- and left-choice reward trials. The activity of these cells was also unaffected by an increase in the number of rewarded trials.

A few reward-directed cells showed both phasic and prolonged responses after reward delivery (Figure 16A). The prolonged responses could correspond to reward intake, as they appeared 0.5 s after the choice and reward and continued for a short time. However, it should be noted that this prolonged activity was dependent on the choice of direction and did not simply reflect the reward intake itself. In contrast, the phasic response corresponded to the sensory input of the reward buzzer and was not dependent on the reward direction. The phasic response could correspond to input from primary sensory pathways, whereas activity during the remaining prolonged time could correspond to

signals from other cortical and/or other areas.

4.3 Interaction between the hippocampus and auditory cortex during the learning process

The activity of reward-direction cells in the hippocampal CA1 reflects positive feedback from the correct port choice to form an association between auditory stimuli and port directions. The proportion of reward-directed cells in the hippocampal CA1 increased in the middle stage and decreased in the late stage of the learning process, whereas on the other hand, the proportion of reward-directed cells in A1 increased in the late stage (Figure 17). According to the two-stage model (Buzsaki, 1996, 2015), the hippocampus could be called the "fast learner," as it rapidly encodes information via changes in synaptic strength during behavioral acquisition. The information is repeatedly replayed during slow-wave sleep and is gradually transferred to the neocortex, resulting in a hippocampal-neocortical interaction that could be referred to as a "slow learning" interaction. Thus, the hippocampus and auditory cortex interact with each other, and the interaction between them plays an important role in memory formation and leads to consolidation (Rothschild et al., 2017). The activity of the reward-direction cells in the A1 may reflect positive feedback, thereby forming and stabilizing auditory associative memories.

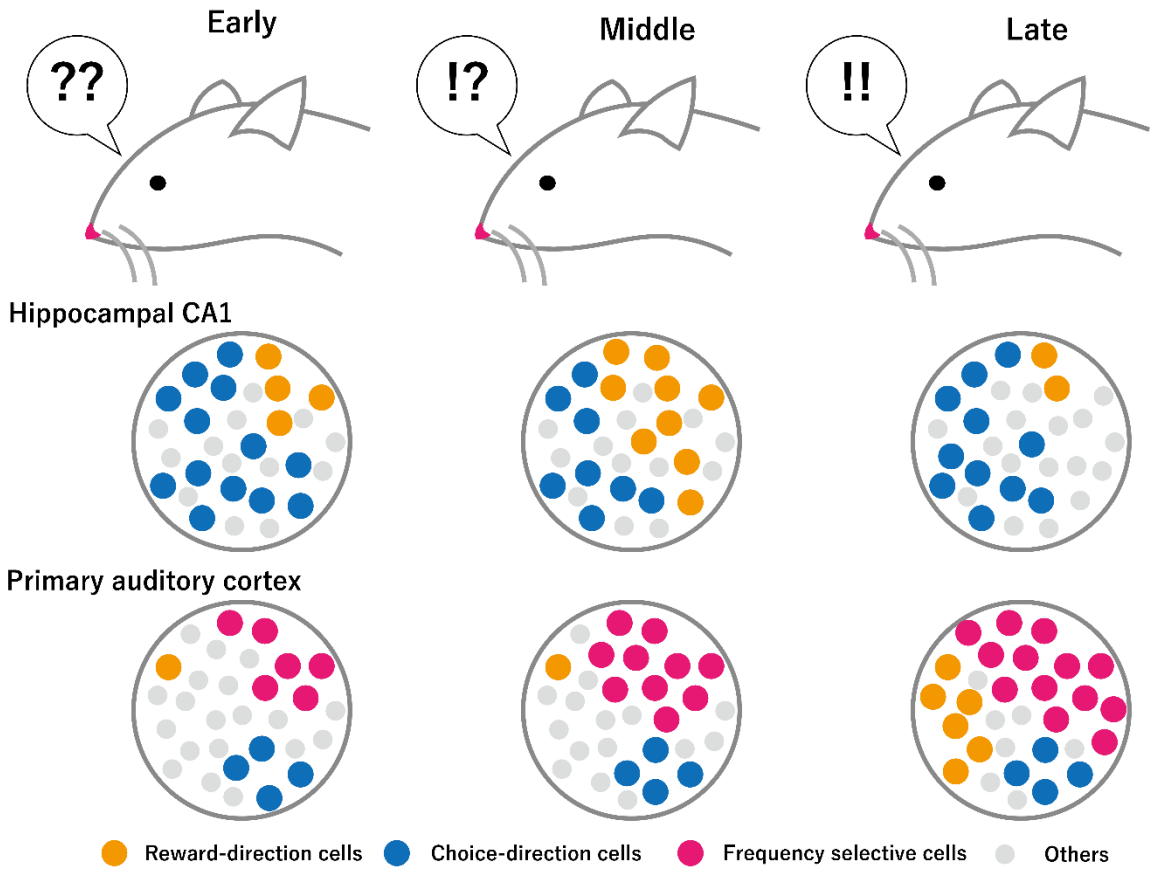

Figure 17. Summary of the results in this study.

The proportion of choice-direction cells in hippocampal CA1 was stable through the learning process. On the other hand, the proportion of reward-direction cells in hippocampal CA1 decreased in the late stage of learning. In A1, the proportions of frequency selective cells and reward-direction cells increased with the learning process. It suggests that hippocampal CA1 neurons play a role as reinforcers during associative learning, and this activity strengthens frequency and reward selectivity in A1 neurons.

There are some pathways between the hippocampus and auditory cortex (Figure 3). However, the role of each pathway is unclear. It is thought that the pathway passing through the entorhinal cortex plays an important role in transferring information from the hippocampus to the auditory cortex. The entorhinal cortex and hippocampus connect to each other, which plays several roles in memory retrieval (Yamamoto et al., 2014) and memory consolidation (Yamamoto and Tonegawa, 2017). Furthermore, the interaction between the hippocampus and entorhinal cortex is strengthened by associative learning (Igarashi et al., 2014).

4.4 Study limitation and future plan

The results of our study indicate that hippocampal CA1 neurons play a role in the acquisition of the association between auditory cues and direction choice. However, no evidence clarifies that the present memory task depends on the hippocampus and that memory retrieval becomes independent from the hippocampus. Further studies are required to reveal the hippocampal dependency of the current task in chemogenetic inactivation studies. This allows us to inactivate a broader range of the hippocampal CA1 neuronal function through time-specific rather than optogenetic or pharmacological studies.

This study could not investigate dynamic modulations of neural activity during the learning process within an individual animal because the number of neurons recorded from an individual was small. We should use high-density electrodes to record neurons at a few hundred orders.

The actual interaction between hippocampal and A1 neurons during the formation and consolidation of auditory associative memory should be examined. The interaction can be observed using LFP coherence, obtained by simultaneous LFP recordings from the hippocampus and auditory cortex with a multi-regional recording system.

The causality between neural activity in the hippocampus and that in A1 during the formation and consolidation of auditory associative memory should be also examined.

To elucidate a role of reward direction selective cells in learning process, experiments with optogenetics might help us. We hypothesize that inactivation of neurons in the hippocampal CA1 in reward epochs causes inhibition of learning progress and modulation of neural activity in A1.

4.5 Outlook

This study showed a probability that hippocampal CA1 neurons play a role as reinforcers during associative learning and that this activity strengthens the frequency and reward selectivity of A1 neurons. The mechanism of associative learning is still unclear. However, our results suggest that the associative learning processes are mediated by reward representation in hippocampal CA1 as a reinforcer and modulation of neural activity in the sensory cortex, influenced by inputs from hippocampal CA1 neurons. These results might help to understand the associative memory mechanism. It is expected that elucidation of the mechanism may lead to the development of efficient learning and behavioral therapy methods for patients with anterograde amnesia.

References

Atiani S., Elhilali M., David S.V., Fritz J.B., Shamma S.A. (2009) Task difficulty and performance induce diverse adaptive patterns in gain and shape of primary auditory cortical receptive fields. *Neuron* **61**: 467-480.

Aoki Y, Igata H, Ikegaya Y, Sasaki T. (2019) The integration of goal-directed signals onto spatial maps of hippocampal place cells. *Cell Reports* **27**: 1516-1527.e5.

Bakin, J. S., Weinberger, N. M. (1990) Classical conditioning induces CS-specific receptive field plasticity in the auditory cortex of the guinea pig. *Brain research* **536**(1-2), 271-286.

Baxter, D. A., Byrne, J. H. (2006) Feeding behavior of Aplysia: a model system for comparing cellular mechanisms of classical and operant conditioning. *Learning & Memory*, **13**(6), 669-680.

Bigelow J., Morrill RJ., Dekloe J., Hasenstaub AR (2019) Movement and VIP interneuron activation differentially modulate encoding in mouse auditory cortex *eNeuro* **6**.

Brosch M, Selezneva E, Scheich H (2011) Representation of Reward Feedback in Primate Auditory Cortex. *Frontiers in Systems Neuroscience* **5**: 1-12.

Buzsáki G. (1996) The hippocampo-neocortical dialogue. *Cerebral Cortex* **6**: 81-92.

Buzsáki, G. (2015) Hippocampal sharp wave-ripple: A cognitive biomarker for episodic memory and planning. *Hippocampus* **25** :1073-188.

Caras M.L., Sanes D.H. (2017) Top-down modulation of sensory cortex gates perceptual learning. *Proceedings of the National Academy of Sciences* **114**: 9972-9977.

Cenquizca, L. A., Swanson, L. W. (2007) Spatial organization of direct hippocampal field CA1 axonal projections to the rest of the cerebral cortex. *Brain research reviews*, **56**(1), 1-26.

David SV, Fritz JB, Shamma SA (2012) Task reward structure shapes rapid receptive field plasticity in auditory cortex. *Proceedings of the National Academy of Sciences* **109**: 2144-9.

De Franceschi G, Barkat TR (2021) Task-induced modulations of neuronal activity along the auditory pathway. *Cell Reports* **37**:11015.

Edeline, J. M., Weinberger, N. M. (1993) Receptive field plasticity in the auditory cortex during frequency discrimination training: selective retuning independent of task difficulty. *Behavioral neuroscience* **107**(1), 82.

Eichenbaum, H., Kuperstein, M., Fagan, A., and Nagode, J. (1987) Cue-sampling and goal-approach correlates of hippocampal unit activity in rats performing an odor-discrimination task. *Journal of Neuroscience* **7**: 716-732.

Eichenbaum, H. (2000) A cortical-hippocampal system for declarative memory. *Nature Reviews Neuroscience* **1**, 41-50.

Felsen, G., Mainen, Z. F. (2008). Neural substrates of sensory-guided locomotor decisions in the rat superior colliculus. *Neuron*, **60**(1), 137-148.

Frankland PW, Bontempi B. (2005) The organization of recent and remote memories.

Nature Reviews Neuroscience **6**: 119-30.

Fritz J., Shamma S., Elhilali M., Klein D. (2003) Rapid task-related plasticity of spectrotemporal receptive fields in primary auditory cortex. *Nature Neuroscience* **6**: 1216-1223.

Fritz J.B., Elhilali M., Shamma S.A. (2005) Differential dynamic plasticity of A1 receptive fields during multiple spectral tasks. *Journal of Neuroscience* **25**: 7623-7635.

Gauthier JL, Tank DW. (2018) A Dedicated Population for Reward Coding in the Hippocampus. *Neuron* **99**: 179-193.

Gershman SJ. (2018) The successor representation: its computational logic and neural substrates. *Journal of Neuroscience* **38**:7193-7200.

Green, D.M., Swets, J.A. (1966) Signal detection theory and psychophysics. New York: Wiley.

Guo, L., Weems, J. T., Walker, W. I., Levichev, A., Jaramillo, S. (2019) Choice-selective

neurons in the auditory cortex and in its striatal target encode reward expectation. *Journal of Neuroscience* **39**(19), 3687-3697.

Hattori S, Chen L, Weiss C, Disterhoft JF. (2015) Robust hippocampal responsivity during retrieval of consolidated associative memory. *Hippocampus* **25**:655-669.

Igarashi KM, Lu L, Colgin LL, Moser M-B, Moser EI. (2014) Coordination of entorhinal–hippocampal ensemble activity during associative learning. *Nature* **510**: 143-147.

Igata H, Ikegaya Y, Sasaki T. (2021) Prioritized experience replays on a hippocampal predictive map for learning. *Proceedings of the National Academy of Sciences* **118**: e2011266118.

Irvine, D. R. (2018) Plasticity in the auditory system. *Hearing research* **362**, 61-73.

Isomura Y, Harukuni R, Takekawa T, Aizawa H, Fukai T. (2009) Microcircuitry coordination of cortical motor information in self-initiation of voluntary movements. *Nature Neuroscience.* **12**: 1586-1593.

Jackson JC, Johnson A, Redish, AD. (2006) Hippocampal sharp waves and reactivation during awake states depend on repeated sequential experience. *Journal of Neuroscience*, **26**(48), 12415-12426.

Kitamura T, Ogawa SK, Roy DS, Okuyama T, Morrissey MD, Smith LM, Redondo RL, Tonegawa S. (2017) Engrams and circuits crucial for systems consolidation of a memory. *Science* **356**: 73-78.

Littman, M. (2015) Reinforcement learning improves behaviour from evaluative feedback. *Nature* **521**: 445-451.

Li Y, Xu J, Liu Y, Zhu J, Liu N, Zeng W, Huang N, Rasch MJ, Jiang H, Gu X, Li X, Luo M, Li C, Teng J, Chen J, Zeng S, Lin L, Zhang X. (2017) A distinct entorhinal cortex to hippocampal CA1 direct circuit for olfactory associative learning. *Nature Neuroscience* **20**: 559-570.

Lin, P. A., Asinof, S. K., Edwards, N. J., Isaacson, J. S. (2019) Arousal regulates frequency tuning in primary auditory cortex. *Proceedings of the National Academy of Sciences* **116**(50), 25304-25310.

Maia TV. (2009) Reinforcement learning, conditioning, and the brain: Successes and challenges. *Cognitive Affective & Behavioral Neuroscience* **9**: 343-64.

McEchron MD, Disterhoft JF. (1997) Sequence of single neuron changes in CA1 hippocampus of rabbits during acquisition of trace eyeblink conditioned responses. *Journal of Neurophysiology* **78**: 1030-1044.

McNaughton, B.L., Battaglia, F.P., Jensen, O., Moser, E.I., and Moser, M.B. (2006) Path integration and the neural basis of the 'cognitive map'. *Nature Reviews Neuroscience* **7**, 663-678.

Miura, K., Mainen, Z. F., Uchida, N. (2012) Odor representations in olfactory cortex: distributed rate coding and decorrelated population activity. *Neuron* **74**(6), 1087-1098.

Modi MN, Dhawale AK, Bhalla UB. (2014) CA1 cell activity sequences emerge after reorganization of network correlation structure during associative learning. *eLife* **3**: e01982.

Mohedano - Moriano, A., Pro - Sistiaga, P., Arroyo - Jimenez, M.M., Artacho - Perula, E., Insausti, A.M., Marcos, P., Cebada - Sanchez, S., Martinez - Ruiz, J., Munoz, M., Blaizot, X. and Martinez - Marcos, A., (2007) Topographical and laminar distribution of cortical input to the monkey entorhinal cortex. *Journal of anatomy*, **211**(2): 250-260.

Momennejad I, Russek EM, Cheong JH, Botvinick MM, Daw ND, Gershman SJ. (2017) The successor representation in human reinforcement learning. *Nature Human Behavior* **1**: 680-692.

Munoz-Lopez, M. M., Mohedano-Moriano, A., Insausti, R. (2010) Anatomical pathways for auditory memory in primates. *Frontiers in neuroanatomy*, **4**, 129.

Nelson A, Schneider DM, Takatoh J, Sakurai K, Wang F, Mooney R (2013) A Circuit for Motor 555 Cortical Modulation of Auditory Cortical Activity. *Journal of Neuroscience* **33**:14342-14353.

O'Keefe, J., and Nadel, L. (1978) The Hippocampus as a Cognitive Map (Oxford University Press).

Ohnuki T, Osako Y, Manabe H, Sakurai Y, Hirokawa J. (2020) Dynamic coordination of the perirhinal cortical neurons supports coherent representations between task epochs. *Communications Biology* **3**: 406.

Olds J, Disterhoft JF, Segal M, Kornblith CL, Hirsh R. (1972) Learning centers of rat brain mapped by measuring latencies of conditioned unit responses. *Journal of Neurophysiology* **35**: 202-219.

O'Mara, S. (2005) The subiculum: what it does, what it might do, and what neuroanatomy has yet to tell us. *Journal of anatomy*, **207**(3), 271-282.

Osako Y, Ohnuki T, Tanisumi Y, Shiotani K, Manabe H, Sakurai Y, Hirokawa J. (2021) Contribution of non-sensory neurons in visual cortical areas to visually guided decisions in the rat. *Current Biology* **19**: S0960-9822(21)00472-3.

Polley, D. B., Steinberg, E. E., Merzenich, M. M. (2006) Perceptual learning directs auditory cortical map reorganization through top-down influences. *Journal of Neuroscience* **26**(18), 4970-4982.

Poo, C., Agarwal, G., Bonacchi, N., Mainen, Z. F. (2021) Spatial maps in piriform cortex during olfactory navigation. *Nature* 1-5.

Recanzone, G. H., Schreiner, C. E., Merzenich, M. M. (1993) Plasticity in the frequency representation of primary auditory cortex following discrimination training in adult owl monkeys. *Journal of Neuroscience* **13**(1), 87-103.

Rothschild, G., Eban, E., Frank, L. M. (2017) A cortical–hippocampal–cortical loop of information processing during memory consolidation. *Nature neuroscience* **20**(2), 251-259.

Rummell BP, Klee JL, Sigurdsson T (2016) Attenuation of Responses to Self-Generated Sounds 563 in Auditory Cortical Neurons. *Journal of Neuroscience* **36**:1201012026.

Sakurai, Y. (1990) Hippocampal cells have behavioral correlates during the performance of an auditory working memory task in the rat. *Behavioral Neuroscience* **104**, 253-263.

Sakurai, Y. (1994). Involvement of auditory cortical and hippocampal neurons in

auditory working memory and reference memory in the rat. *Journal of Neuroscience*, **14**(5), 2606-2623.

Sakurai Y. (1996) Hippocampal and neocortical cell assemblies encode memory processes for different types of stimuli in the rat. *Journal of Neuroscience* **16**, 2809-2819.

Schmitzer-Torbert NC, Jackson J, Henze D, Harris K, Redish AD. (2005) Quantitative measures of cluster quality for use in extracellular recordings. *Neuroscience* **131**:1-11.

Shiotani K, Tanisumi Y, Murata K, Hirokawa J, Sakurai Y, Manabe H. (2020) Tuning of olfactory cortex ventral tenia tecta neurons to distinct task elements of goal-directed behavior. *elife* **9**: e57268.

Siegel, S. (1956) Nonpararnetric Statistics : For the Behavioral Sciences. New York: McGraw-Hill.

Skinner, B. F. (1937) Two types of conditioned reflex: A reply to Konorski and Miller. *The Journal of General Psychology*, **16**(1), 272-279.

Squire, L. R. Memory and Brain. Oxford University Press, Oxford (1987).

Stachenfeld KL, Botvinick MM, Gershman SJ. (2017) The hippocampus as a predictive map. *Nature Neuroscience* **20**: 1643-1653.

Stringer, C., Michaelos, M., Tsyboulski, D., Lindo, S. E., Pachitariu, M. (2021) High-precision coding in visual cortex. *Cell* **184**(10), 2767-2778.

Tanisumi Y, Shiotani K, Hirokawa J, Sakurai Y, Manabe H. (2021) Bi-directional encoding of context-based odors and behavioral states by the nucleus of the lateral olfactory tract. *iScience* **24**: 102381.

Terada S, Sakurai Y, Nakahara H, Fujisawa S. (2017) Temporal and Rate Coding for Discrete Event Sequences in the Hippocampus. *Neuron* **94**: 1248-1262.e4.

Tse, D., Langston, R. F., Kakeyama, M., Bethus, I., Spooner, P. A., Wood, E. R., Witter, M.P., Morris, R. G. (2007). Schemas and memory consolidation. *Science*, **316**: 5821, 76-82.

Weinberger, N. M. (2004) Specific long-term memory traces in primary auditory cortex. *Nature Reviews Neuroscience* **5**(4), 279-290.

Wirth S, Yanike M, Frank LM, Smith AC, Brown EN, Suzuki WA. (2003) Single neurons in the monkey hippocampus and learning of new associations. *Science* **300**: 1578-1581.

Yamamoto, J., Suh, J., Takeuchi, D., Tonegawa, S. (2014) Successful execution of working memory linked to synchronized high-frequency gamma oscillations. *Cell*, **157**(4), 845-857.

Yamamoto, J., Tonegawa, S. (2017) Direct medial entorhinal cortex input to hippocampal CA1 is crucial for extended quiet awake replay. *Neuron*, **96**(1), 217-227.